COASTAL IFOA MONITORING PROGRAM

Quantification and Monitoring of Sudden Canopy Dieback in Forests of the North Coast of NSW – Final Report

June 2025

A report submitted to the NSW Natural Resources Commission.

Acknowledgement of Country

With respect for Aboriginal cultural protocol and out of recognition that its campuses occupy their traditional lands, Western Sydney University acknowledges the Darug, Eora, Dharawal (also referred to as Tharawal) and Wiradjuri peoples and thanks them for their support of its work in their lands (Greater Western Sydney and beyond). Western Sydney University conducted field surveys on the lands of the Kurnai, Bidwell, Yuin, Ngunawal, Gundungurra, Wiradjuri, Dharug, Darkinung, Dainggatti, Gumbainggir and Ngarabal peoples. Western Sydney University also acknowledges and pays respects to Elders past and present.

Acknowledgements

Western Sydney University acknowledges and appreciates the assistance, support and feedback provided by the Natural Resources Commission, Forestry Corporation of NSW, and Jason MacKenzie.

Disclaimer

This document contains development of methodology to monitor canopy dieback based on remote sensing and ground-based observations. The Authors will not accept responsibility or be liable for any consequences that arise directly or indirectly from using the information contained within this document.

Citation:

Choat, B., Nolan, R. H., Quan, X., Gibson, R.K. (2025) *Quantification and Monitoring of Sudden Canopy Dieback in Forests of the North Coast of NSW, Final Report* Hawkesbury Institute for the Environment, Western Sydney University.

Contents

GLOSSARY OF ACRONYMS

Acronym	Full Term
AOI	Area of Interest
BMAD	Bell Miner Associated Dieback
CIFOA	Coastal Integrated Forestry Operations Approvals
CV	Coefficient of Variation
CR	Change Rate
DEM	Digital Elevation Model
DBH	Diameter at Breast Height
FESM	Fire Extent and Severity Mapping
GEE	Google Earth Engine
GVMI	Global Vegetation Moisture Index
LFMC	Live Fuel Moisture Content
LightGBM	Light Gradient Boosting Machine Learning Model
MATLAB	Matrix Laboratory (software by MathWorks)
MSI	Moisture Stress Index
MTCI	MERIS Terrestrial Chlorophyll Index
NDII	Normalized Difference Infrared Index
NDVI	Normalized Difference Vegetation Index
OSAVI	Optimized Soil-Adjusted Vegetation Index
QGIS	Quantum Geographic Information System
RERI705	Red Edge Relative Index (band 705)
RERI783	Red Edge Relative Index (band 783)
RF	Random Forest Model
RGB	Red Green Blue (bands in imagery)
RTM	Radiative Transfer Model
SHAP	Shapley Additive exPlanations
SPEI	Standardized Precipitation and Evapotranspiration Index
SWIR	Shortwave Infrared
TCARI	Transformed Chlorophyll Absorption in Reflectance Index
TPI	Topographic Position Index
TWI	Topographic Wetness Index
UTM	Universal Transverse Mercator
VI(s)	Vegetation Index/Indices
WSU	Western Sydney University
WGS 84	World Geodetic System 1984

1. General Introduction

1.1. Report Context

The Coastal Integrated Forestry Operations Approval (CIFOA) is designed to deliver ecologically sustainable forest management in NSW forests, securing a long-term forestry industry, and establishing credible, effective and enforceable environmental regulations for forestry operations (EPA n.d.). The CIFOA requires that a monitoring program is applied at multiple landscape scales to ensure the ongoing effectiveness of the approval in achieving these outcomes. The Natural Resources Commission (the Commission) oversees the implementation of the Coastal IFOA monitoring program (the program) on behalf of the NSW Forest Monitoring Steering Committee.

The program developed a series of monitoring plans including for forest structure, health and regeneration, for which one of the monitoring questions is "*To what extent are the [CIFOA] conditions effectively managing the risk of new or existing areas subject to dieback?*"

No existing cost-effective methods were identified to monitor areas subject to dieback at the landscape scale. Hence, the current project was established to develop a scientifically robust method to assess canopy dieback and how this can be related to potential causal factors.

1.2. Report Summary

The study was initiated as part of the Coastal Integrated Forestry Operations Approval (CIFOA) Monitoring Program to develop a scientifically robust method to assess canopy dieback and how this can be related to potential causal factors. With extreme climate events becoming more frequent, particularly prolonged droughts and high-intensity bushfires, understanding the spatial extent and drivers of canopy dieback is critical for the future management of NSW forest ecosystems. This report describes the method developed and its use to investigate the widespread canopy dieback observed in eucalypt dominated forests of the NSW North Coast following a severe early-season drought in September–October 2023.

To achieve this, the study employed a combination of remote sensing, machine learning, and ground-based surveys. High-resolution PlanetScope imagery was used to manually classify canopy conditions into three categories: dead, partially dead, and live. This classification was then extended across the broader study area using Sentinel-2 imagery and a machine learning approach based on a Random Forest model, which achieved an accuracy of 94–96% in predicting the severity of canopy dieback in test areas of interest. A further analysis was done to assess the influence of topography, fire history, and land management on canopy dieback patterns using LightGBM models and SHAP values. Ground-based surveys were done at selected sites to assess longer-term impacts on tree health resulting from different classes of canopy dieback.

The results demonstrated that canopy dieback was most extensive on ridges and north-facing slopes. It is likely that higher solar radiation and reduced soil moisture retention increased drought stress in these terrain positions. Analysis of the Topographic Position Index (TPI) confirmed that exposed upper slopes were more likely to experience full and partial canopy dieback, whereas lower-lying gullies, which are predicted to retain more moisture, exhibited less canopy dieback. The Topographic Wetness Index (TWI) further indicated that drier areas were more susceptible to full canopy dieback, although the relationship between partial canopy dieback and TWI was ambiguous.

Previous fire history was also a strong predictor of canopy dieback patterns. Areas that burned at high or extreme severity during the 2019-2020 Black Summer fires showed a strong likelihood of experiencing further canopy dieback in 2023, suggesting a legacy effect of past disturbance. In these areas, tree recovery from fire may be limited, making them more vulnerable to subsequent drought stress. Land management history also influenced dieback severity. National Parks and other protected areas outside of State Forests exhibited the highest probability of full canopy dieback. State Forests managed for harvest had the lowest probability of full canopy dieback but exhibited the highest probability of partial dieback, indicating that while they were less likely to experience complete mortality, they remained vulnerable to moderate canopy stress. Areas previously impacted by Bell Miner Associated Dieback (BMAD) had high levels of canopy dieback, but the area affected was small compared to other factors associated with canopy dieback. Further analysis using more detailed land management history is needed to understand these outcomes.

A time-series analysis from 2019 to 2023 revealed multiple peaks in canopy dieback, with the most significant occurring in late 2019, following the Black Summer fires, and in late 2023, during the most recent drought. Although satellite imagery suggested some degree of canopy recovery after drought events, ground-based surveys confirmed that areas classified as dead canopy in 2023 contained a significantly higher proportion of dead trees one year later. Surveyed plots in ridge-top positions exhibited the greatest tree mortality, while gully and south-facing slope plots showed better recovery. These findings suggest that while some forested areas may recover visually in remote sensing data, the ecological impact of dieback events may persist for years, with long-term consequences for forest structure and species composition.

Based on these findings, the study recommends expanding dieback mapping efforts across a broader region to improve early detection and response. Further refinement of tree-level monitoring is also suggested, incorporating LiDAR and high-resolution aerial imagery to track individual tree crown dynamics more accurately. Establishing permanent ground survey plots will be essential to validate remote sensing results and monitor long-term recovery trends. Additionally, forest management strategies should integrate dieback risk into decision-making.

This study provides a comprehensive methodology for mapping and monitoring canopy dieback and highlights the complex interactions between drought, fire history, and topographic factors. The results underscore the need for continued monitoring, predictive modelling, and adaptive forest management to mitigate the risks associated with climate-driven forest decline.

1.3. Introduction

1.3.1. Forest Mortality and Dieback

Tree dieback is a global issue linked to a range of interdependent causal factors including drought stress, heat waves, storms, pests, pathogens, and bushfires (Allen et al. 2010). Drought stress is the most widespread factor associated with tree dieback, with the potential to kill millions of trees in relatively short timescales (Choat et al. 2018; McDowell et al. 2022). Although key components of the Australian woody flora have evolved with drought, increasing temperatures and a higher frequency of extreme weather events have led to elevated risk of widespread forest dieback in Australian forests. The climate of south-eastern Australia is characterised by large interannual variability in rainfall, leading to periodic severe droughts that develop over multiyear periods (Nicholls 1991). While it is difficult to predict future rainfall patterns with certainty, the background increase in air temperature will generally lead to higher evaporative demand and evapotranspiration from plants and soils. This means that plant water stress is likely to set in earlier, and reach a higher intensity, during a given period of below average rainfall (Trenberth et al. 2014). The shortening return interval and compounding nature of disturbance events has the potential to cause higher levels of tree mortality and canopy dieback. Evidence of elevated canopy dieback and tree mortality related to drought and heat has already been observed in NSW forests (Nolan et al. 2021; Losso et al. 2022), raising concerns regarding the role of land management strategies and possible interaction with other causal factors.

In NSW, the record 2017-20 drought caused broad scale canopy dieback in eucalypt species across all major forest and woodland vegetation types (Losso et al. 2022). Physiological measurements on affected trees indicated that the primary cause of dieback during the drought was failure of the plant hydraulic system caused by the development of extreme water stress (Nolan et al. 2021). This drought event also led to increased forest flammability and was a primary causal factor in the catastrophic Black Summer bushfires, which burned over 5 million hectares of native forests in NSW alone (Boer et al. 2020).

The following years have delivered record rainfall, alleviating soil water deficits and allowing recovery across the majority of NSW forest and woodland systems. However, recovery has been staggered (Losso et al. 2022; Nichols et al. in prep), most likely due to legacy effects from drought and fires, along with soil water logging caused by extreme rainfall events. NSW experienced a period of below average rainfall coupled with higher than average temperatures from May to October of 2023. Based on climate deciles, rainfall was very much below average and maximum temperatures were the highest on record for the majority of the State during this period. Modelled root zone moisture was in the lowest 1% percentile rank for September and October for the North Coast region prior to rainfall in November that facilitated rapid recovery (Fig. 1). Short duration drought events such as this are referred to as ‘flash droughts’ (Christian et al. 2024). For the purposes of this report, we define drought with the standardised precipitation and evapotranspiration index (SPEI), which uses both precipitation and evapotranspiration data to quantify the climatic water balance (Vicente-Serrano et al., 2010). As suggested by Rhee and Im (2017), SPEI thresholds can be used to define drought status as follows: moderate drought ($-1.49 \leq \text{SPEI} \leq -1$), severe drought ($-1.99 \leq \text{SPEI} \leq -1.5$), extreme drought ($\text{SPEI} \leq -2$). Based on these definitions and 6-month SPEI values, the North Coast region was in severe drought from September to November of 2023. This early-season drought event caused rapid and extensive canopy dieback in the coastal ranges of northern NSW (Fig. 2). The dieback event was noted by NSW government agencies, forestry staff, and community groups; many records were submitted to the citizen science project the dead tree detective (Atlas of Living Australia, 2024). However, the extent and patterning of recent dieback events has not been quantified.

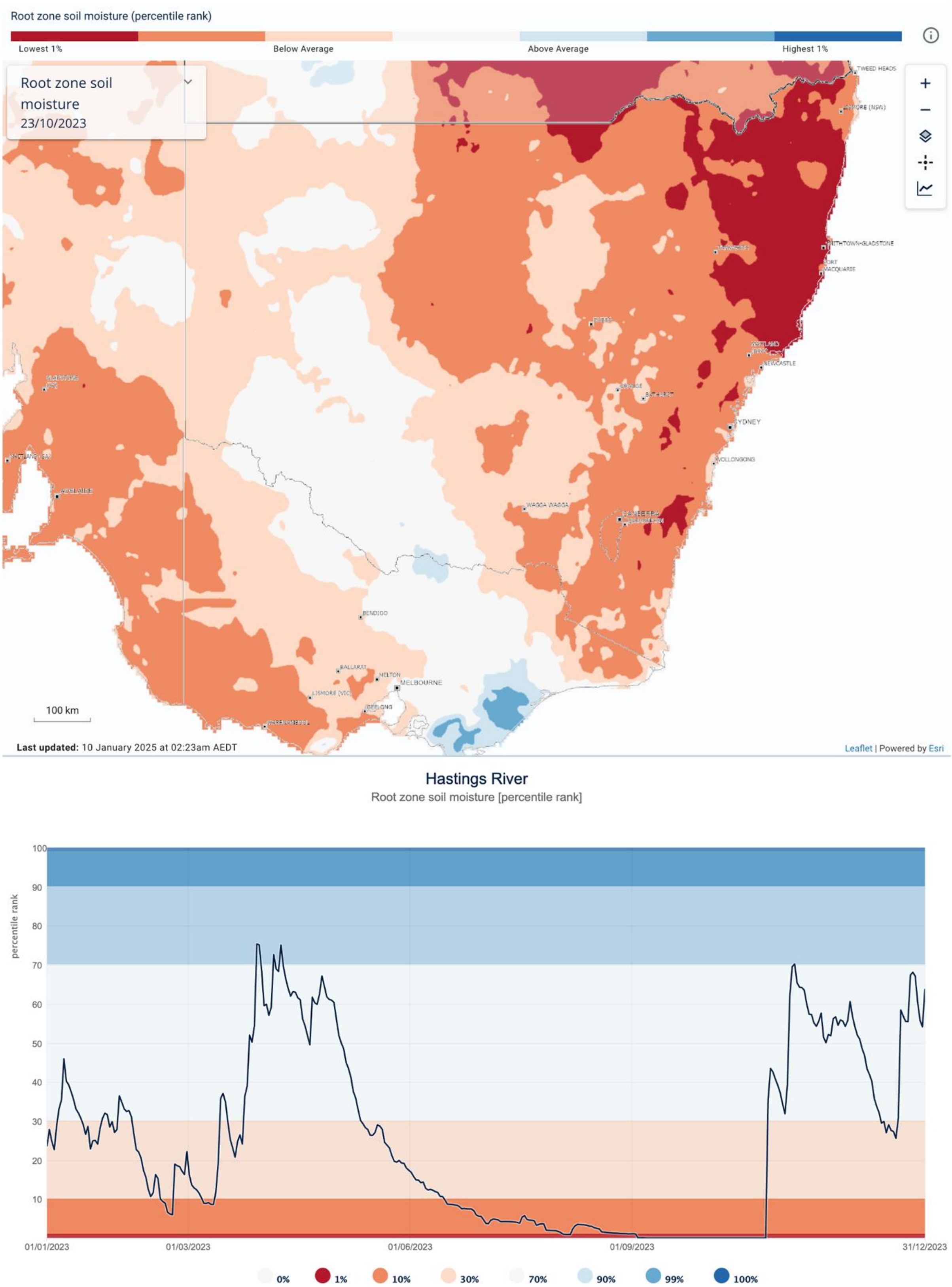

Figure 1. (A) Root zone soil moisture estimated for NSW on 23/10/2023 showing predicted soil moisture in the lowest one percent of values for the NSW North Coast region (B) Change in percentile rank of predicted root zone soil moisture across 2023 for the Hastings River area. Source: Australian Water Resource Assessment Landscape model.

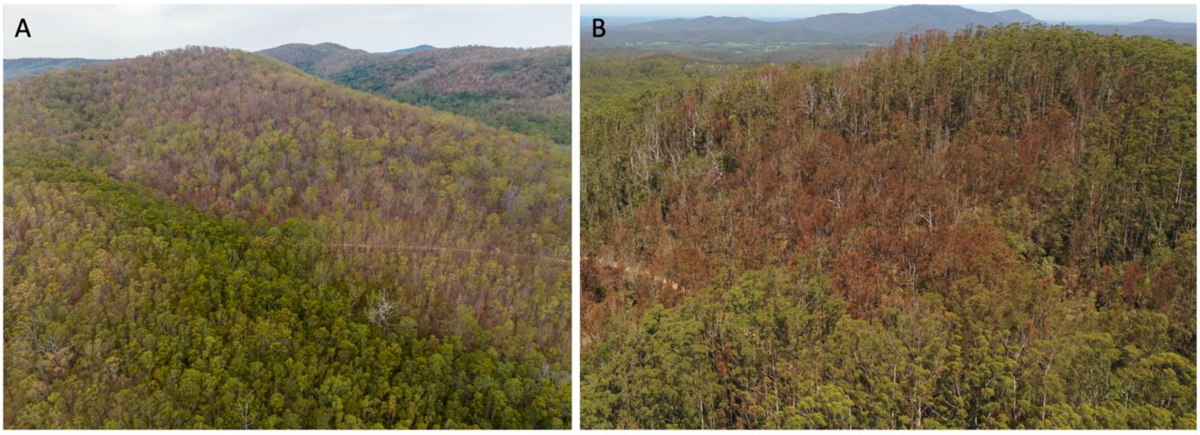

Figure 2. Examples of widespread canopy dieback observed in the NSW North Coast region in October and November of 2023. Photo credits (A) Brendan Bernie (B) Matthew Nagel.

1.3.2. Causes and Consequences of Drought Associated Dieback in NSW

During drought, reduced precipitation leads to declines in soil moisture, which are often accompanied by higher temperatures and increased evaporative demand from the atmosphere. These factors combine to induce water stress in plants, which is manifested as increased tension in the xylem sap. Soil water deficit caused by drought may be exacerbated by extreme temperatures because trees must close their stomata to restrict water loss and delay drought induced injury (Landsberg and Waring 2017). However, stomatal closure leads to rapid declines in photosynthesis and a reduction in evaporative cooling that may push leaves beyond their thermal limits (Leigh et al., 2017). With increasing plant water stress, the plant hydraulic system (xylem) will begin to fail, leading to tissue death throughout the plant, including canopy, branches, and roots. Ultimately, drought may cause (i) partial dieback of a tree, which may then recover when drought stress is relieved by rainfall, or (ii) whole plant mortality. Canopy dieback is distinct from whole plant mortality; canopy dieback describes the partial or full loss of foliage and branches in the tree's canopy, while the tree remains alive. Tree mortality describes the complete death of a tree, including all above- and below-ground tissues. Eucalypt species may recover from canopy dieback by re-initiation of apical meristems and regrowth from epicormic buds once favourable plant water status is restored (Nolan et al. 2014; Bendall et al. 2022). In some cases, the whole above ground biomass of the tree is killed and trees recover via basal resprouting from lignotubers. The root system is also damaged by drought but the extent of dieback below ground is more difficult to observe and has thus not been well documented. In eucalypt dominated forests, widespread canopy dieback associated with severe stress events typically results in increased whole tree mortality (Nolan et al. 2022; Bendall et al. 2024). Tree mortality is more difficult to diagnose than canopy dieback and can only be confirmed 1-2 years after stress events, where bark is lost from trees and no resprouting occurs from the trunk or lignotuber.

The impacts of drought stress are likely to render trees more vulnerable to mortality during and after drought, through interactions with other causal agents such as fire, pests, and pathogens. For instance, reduced water content in the leaves, bark, and wood may lead to higher levels of injury during fires (Bendall et al. 2024). The imposition of drought stress on native tree species may also affect post-fire recovery. Most eucalypts recover from fire via resprouting, however, leaves and branches developing from epicormic buds may be more vulnerable to drought stress, leading to extensive dieback of epicormic tissue if drought stress is imposed post-fire. In this way, cumulative stress may also deplete the carbohydrate reserves of recovering trees, leading to increased chance of mortality in the longer term (Smith et al 2018).

Drought will also cause a reduction in resources available for defence, rendering trees more vulnerable to pests and pathogens (Landsberg and Wylie 1983). This is thought to be the case for woodboring Longicorn beetle (*Phoracantha* sp.) responsible for Snow Gum dieback in the Australian Alps (Bryant et al. 2024). Other modes of dieback identified in NSW, such as Bell Miner Associated Dieback (BMAD), may also be exacerbated by drought stress since trees weakened by psyllids are likely more susceptible to drought-induced dieback. Activity of soil fungal pathogens such as *Phytophthora* may also be influenced by water and heat stress; although the pathogen is most active in moist soils, stress associated with drought may predispose trees to root rot with heavy rainfall. However, *Phytophthora* is generally not regarded as a significant threat to vegetation in NSW (McDougall and Summerell 2001).

1.3.3. Monitoring and Mapping Tree Dieback

Accurate monitoring and mapping of canopy dieback is essential to understand the impacts of dieback on forest systems and the interaction of causal factors associated with these events. While drought is clearly the major proximal cause of canopy dieback in this case, other factors such as topography, fire history, management practices, pests, and pathogens are likely to drive the complex spatial patterning of dieback observed in the landscape. In NSW, mapping of canopy dieback has been undertaken using a range of ground based and remote sensing methodologies. This includes mapping of canopy dieback associated with fire and drought using spectral indices derived from satellite imagery (Hislop et al. 2023), ground surveys documenting the impacts of drought on canopy health (Losso et al. 2022), and aerial surveys of dieback associated with BMAD (Silver and Carnegie 2017). While ground surveys offer accurate information on the health status of individual trees within small plots, assessment of the full extent of dieback at local and regional scales requires remote sensing data. In addition, ground based surveys provide essential data for validation and training of remote sensing products.

Significant effort was invested into mapping fire severity impact in NSW vegetation after the 2019-2020 bushfire season; the tools and methods used can also be used for mapping the severity of recent drought-induced damage. Gibson et al. (2020) utilized spectral indices from the Sentinel-2 satellite platform and machine learning approaches to classify the severity of fire impacts in NSW. The results of this study indicated that fire severity could be mapped with very high accuracy using Sentinel-2 imagery and supervised classification by a machine learning framework (Random Forest). Using a combination of high-resolution satellite imagery and machine learning may provide an opportunity to more accurately and cost effectively map canopy dieback associated with drought and other causal factors in NSW forests. Measuring the impact of disturbance on forest canopies may also be improved by the use of LiDAR, which provides information on changes in canopy structure that complement spectral data derived from satellites. If collected at multiple timepoints and sufficient spatial resolution, LiDAR can be used to effectively monitor rates of tree mortality and recovery of surviving individuals. This is particularly valuable since recovery of trees is difficult to monitor with spectral data alone, because of a confounding greenness signal coming from rapid growth of grass or shrub layers under the canopy of impacted trees.

Accurate mapping methods also allow for attribution analysis to understand the impacts of management practices and other potential causal factors on the occurrence and patterning of dieback in the landscape. In this report we detail a methodology to monitor canopy dieback in NSW forests and to determine the factors governing variation in dieback observed across the landscape.

1.4. Aims

The overarching aim of this pilot study was to develop a methodology for mapping canopy dieback in forested areas of NSW to help understand the role of causal factors in controlling the patterns and extent of dieback observed. The project focused on the extensive canopy dieback that occurred in September to October of 2023 as a case study. Specific aims include:

1. Evaluate potential of high-resolution satellite imagery to quantify historical and recent canopy dieback for the 2023 September-October drought in selected areas.

2. Produce a full extent map for a case-study area using the output from Aim 1 as training data to model dieback severity using Sentinel-2 imagery.

3. Determine current canopy condition, basal area of dead trees, and causal factors associated for canopy dieback by ground surveys at selected sites.

4. Investigate patterns of drought-induced dieback in relation to other causal factors such as topography, fire history, forestry operations, and land management.

2. Methodology

2.1. Study Area

The pilot study focused on a sudden dieback event associated with an early season drought that peaked in September and October of 2023. Based on initial exploration of PlanetScope satellite imagery during the September to October period, it was determined that the extent of canopy dieback was greatest in forest estates immediately north and south of Port Macquarie and in the region surrounding Grafton. Canopy dieback was far less visible in the forests surrounding Coffs Harbour and in forests of the NSW South Coast region. The area of interest (AOI) for this study was designed to capture clear evidence of multiple dieback response stages (i.e., “live”, “partial” and “dead”) across public lands on the North Coast of NSW. Public lands vary in terms of management objectives and interventions occurring in harvested state forests versus protected conservation areas.

We identified three sub-AOIs within the full extent North Coast AOI that encompasses forest estates with a range of tenures (State Forests, Nature Reserves, National Park) and management zones (Fig. 3). Large areas of forest within this region had also been severely burnt in the Black Summer fires of 2019-2020. Remotely sensed products and auxiliary data were acquired or derived for a regional footprint of 11,709 km^2 that includes the three sub-AOIs.

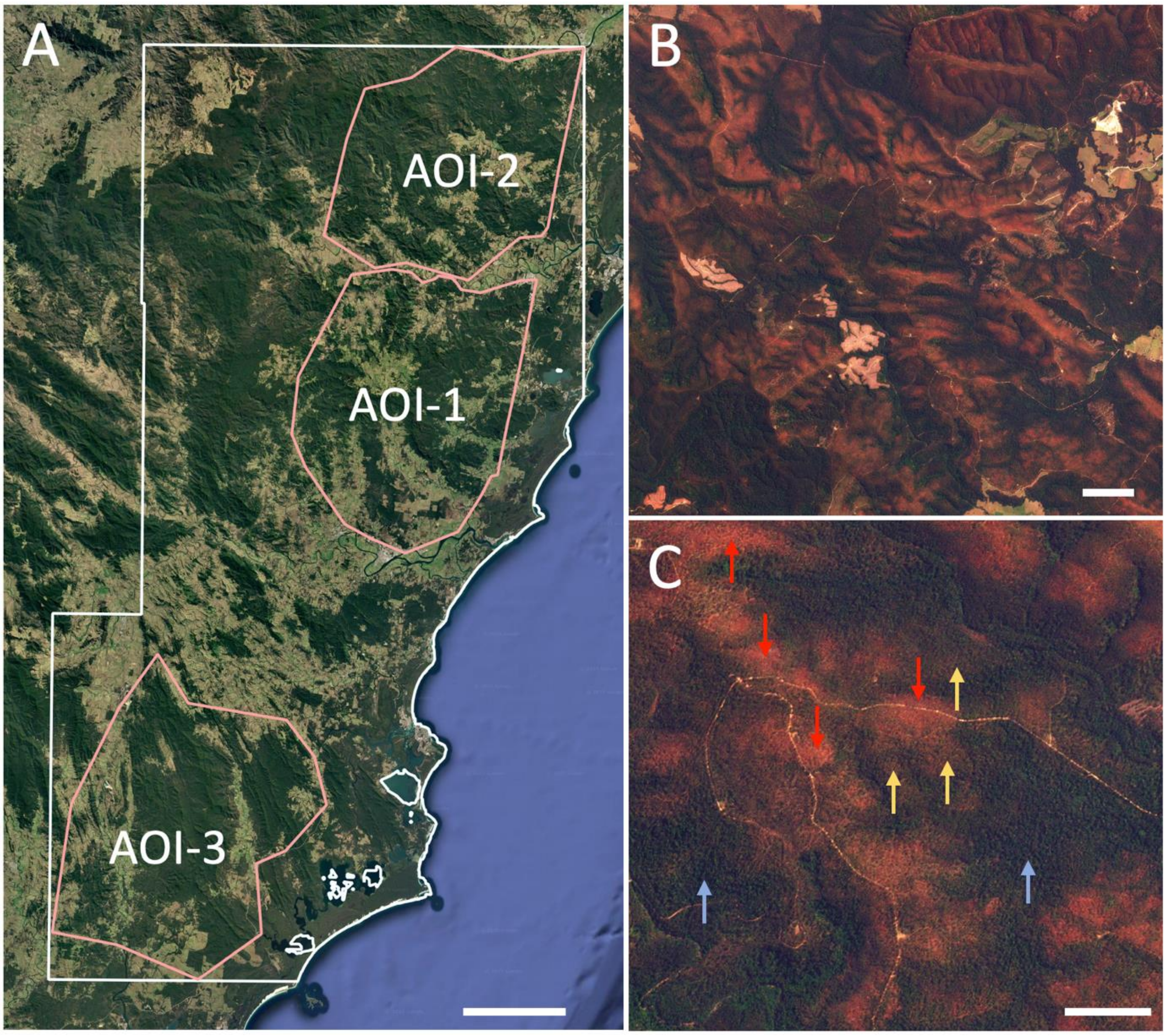

Figure 3. (A) Area of NSW North Coast used in the study. The white bounding box shows the full extent of the area of interest in which canopy dieback was examined. Smaller bounding areas show the sub-AOIs used for generation of hand digitisation and training data. PlanetScope 3m imagery was downloaded for the three sub-Areas of Interest (AOI-1, 2, 3) shown. (B) Example of canopy dieback visualisation during October 2023 from within AOI-1. (C) Closer view showing examples of dead canopy (red arrows), partially dead canopy (yellow arrows), and live canopy (blue arrows). Scale bars indicate 20 km, 1 km and 0.5 km for A, B and C, respectively.

2.2. Processing and Analysis of Satellite Imagery

Processing, analysis, and modelling of spatial data was primarily conducted in R version 4.4.2 (R Core Team 2024) and MATLAB version 9.13.0 R2024b (MathWorks 2024), with visualisation and cartographic support by ArcGIS Pro (ESRI 2024) and QGIS (QGIS.org 2024). All spatial data were projected (epsg:32756; WGS 84 / UTM zone 56S) and clipped to the AOI using MATLAB.

2.3. Use of High-Resolution Satellite Imagery to Quantify Canopy Dieback

Orthorectified PlanetScope Imagery for each of the three AOIs was used to generate hand digitised spatial polygons defining sample areas of canopy dieback. PlanetScope supplies 3 m/pixel resolution images in four multispectral bands (RGB and Near Infrared) from a fleet of 200 CubeSats. This imagery is available at daily return intervals, making it ideal for identification of canopy dieback in eucalypt forests. PlanetScope Ortho Analytical 4B SR scenes (i.e., orthorectified, surface reflectance 4-band image products suitable for analysis) were downloaded for the three AOIs at two timepoints: 'pre-drought' and 'post-drought'. For remotely sensed evidence of dieback, peak occurrence of dieback occurred 'post-drought' in October 2023, whereas for comparative purposes, 'pre-drought' is defined here as October 2022. The exact dates used from each year were selected to provide the greatest visible area, i.e. the date of 23/10/2023, which provided 100% cloud free imagery for each sub-AOI. This high resolution multi-spectral imagery was used to manually label polygons representing three stages of dieback (1) dead canopy, (2) partial dead canopy, (3) live canopy (see Table 1 and Fig. 3C) in QGIS (Version 3.34). Dead canopy refers to a canopy that appears completely brown at the pixel level in PlanetScope imagery. Partial dead canopy describes a canopy with a mix of green and brown foliage. Live canopy refers to a canopy that appears entirely green.

Table 1. Description of canopy dieback classes used to map dieback severity, with example polygons used to manually classify dieback classes using PlanetScope imagery.

Canopy Dieback Class	Description	Example Polygon
Dead canopy	Canopy entirely brown	
Partial dead canopy	Canopy mix of brown and green	
Live canopy	Canopy entirely green	

In this case, canopy dieback is differentiated from whole tree mortality. While canopy dieback can be identified from high resolution satellite imagery and aerial surveys, accurate assessment of tree mortality in eucalypt species requires ground-based surveys at some time after a disturbance event has occurred. As such, canopy dieback refers to browning of leaves and loss of canopy that occurs during a disturbance event that may lead to tree morality. However, many eucalypt trees that experience full canopy dieback can recover via epicormic resprouting if favourable growth conditions allow it. Polygons were also labelled to define grassland and bare ground to assist with training and classification. Labels (manually classified polygons) were designed for use in both classification and regression models (described below). Only areas of continuous forest were considered; paddock trees and small patches of trees were excluded from analysis. A shapefile layer was generated containing polygons for each of the five canopy classes. Imagery from dates before the dieback event was used to determine whether areas exhibiting canopy dieback were impacted prior to the Sept-Oct 2023 drought.

2.4. Full Extent Mapping of Canopy Dieback in Case Study Area

While PlanetScope offers high resolution imagery at short return intervals, it is not freely available and therefore not well suited for analyses at regional or statewide scales. We instead used hand digitization of PlanetScope imagery to generate training data for a machine learning based approach to mapping canopy dieback across the full extent of the case study area. In this case, we selected the Random Forest (RF) model to allow for supervised classification of canopy dieback classes using freely available data from Sentinel-2 satellites. A similar approach has previously been used to map fire severity in southeast Australia (Gibson et al. 2020).

2.4.1. Sentinel-2 Spectra and Derived Indices

Monthly Sentinel-2A/2B surface reflectance data were acquired from the Google Earth Engine (GEE) platform (Gorelick et al. 2017) for the period between January 2019 and October 2023. To ensure data quality, images with a cloud probability of less than 10% were selected, and the monthly median reflectance value for each pixel was calculated from the filtered dataset. All imagery and spectral bands were resampled to a 10 m spatial resolution using the GEE platform. Although the spatial resolution of Sentinel-2 imagery (10 m) is lower than that of PlanetScope (3 m), it offers significant advantages due to its free accessibility and rich spectral information. With wavebands spanning optical, near-infrared, and shortwave infrared regions, Sentinel-2 data are well-suited for estimating live fuel moisture content (LFMC) and deriving multiple greening indices related to canopy pigment. These attributes make it a robust resource for regional-scale canopy dieback mapping.

2.4.2. Selected Vegetation Indices

We evaluated the sensitivity of 12 vegetation indices (VIs) to map canopy dieback severity across the case study area. Vegetation indices were derived from Sentinel-2 imagery and could be divided into two categories, chlorophyll-related VIs and leaf water-related VIs. The chlorophyll-related VIs included transformed chlorophyll absorption in reflectance index (TCARI), optimized soil-adjusted vegetation index (OSAVI), ratio R740/R705, ratio R865/R665, two Red Edge Relative Indices (RERI705 and RERI783), normalized difference vegetation index (NDVI), and Envisat MERIS Terrestrial Chlorophyll Index (MTCI). These indices contain red bands that are sensitive to chlorophyll content. The leaf water-related VIs or variables included the normalized difference infrared index (NDII) (with the same formula as the normalized burn ratio, NBR), the global vegetation moisture index (GVMI), and moisture stress index (MSI). These indices include the shortwave infrared band (SWIR) that is sensitive to leaf water content. Formulas for calculating VIs are provided below:

$$\mathrm{TCARI} = 3\left[(\mathrm{R}_{705} - \mathrm{R}_{665}) - 0.2(\mathrm{R}_{705} - \mathrm{R}_{560})\left(\frac{\mathrm{R}_{705}}{\mathrm{R}_{665}}\right)\right] \tag{1}$$

$$\mathrm{OSAVI} = \frac{(1 + 0.16)(\mathrm{R}_{865} - \mathrm{R}_{665})}{\mathrm{R}_{865} + \mathrm{R}_{665} + 0.16} \tag{2}$$

$$\mathrm{RERI}_{705} = \frac{\mathrm{R}_{705} - \mathrm{R}_{665}}{\mathrm{R}_{865}} \tag{3}$$

$$\mathrm{RERI}_{783} = \frac{\mathrm{R}_{783} - \mathrm{R}_{705}}{\mathrm{R}_{865}} \tag{4}$$

$$\mathrm{NDVI} = \frac{\mathrm{R}_{NIR} - \mathrm{R}_{red}}{\mathrm{R}_{NIR} + \mathrm{R}_{red}} \tag{5}$$

$$\mathrm{MTCI} = \frac{\mathrm{R}_{753.75} - \mathrm{R}_{708.75}}{\mathrm{R}_{708.75} + \mathrm{R}_{681.25}} = \frac{\mathrm{R}_{band6} - \mathrm{R}_{band5}}{\mathrm{R}_{band5} + \mathrm{R}_{band4}} \tag{6}$$

$$\mathrm{NBR} = \frac{\mathrm{R}_{NIR} - \mathrm{R}_{SWIR1}}{\mathrm{R}_{NIR} + \mathrm{R}_{SWIR1}} \tag{7}$$

$$\mathrm{GVMI} = \frac{(\mathrm{R}_{NIR} + 0.1) - (\mathrm{R}_{SWIR1} + 0.02)}{(\mathrm{R}_{NIR} + 0.1) + (\mathrm{R}_{SWIR1} + 0.02)} \tag{8}$$

$$\mathrm{MSI} = \frac{\mathrm{R}_{SWIR1}}{\mathrm{R}_{NIR}} \tag{9}$$

2.4.3. Derivation of Live Fuel Moisture Content

In addition to the 11 VIs derived directly from spectral data, we estimated Live Fuel Moisture Content (LFMC) from satellite data. Live Fuel Moisture Content is the ratio of vegetation water content to its dry weight:

$$\mathrm{LFMC} = \frac{W_{fresh} - W_{dry}}{W_{dry}} \times 100\% \tag{10}$$

Where W_{fresh} is the fresh weight of the leaf and W_{dry} is the leaf dry weight. Live fuel moisture content can be measured directly on leaves collected from the field but may also be estimated from remotely sensed data and a Radiative Transfer Model (RTM). In this case, LFMC estimation was based on the methodology presented in previous studies (Quan et al. 2024; Quan et al. 2021; Yebra et al. 2018). While previous studies have commonly used MODIS data with a spatial resolution of 500 m to estimate LFMC, here we used Sentinel-2 data with a 10 m resolution. Briefly, the LFMC was retrieved through radiative transfer model inversions from the Sentinel-2A/B reflectance product obtained from the GEE platform. The RTMs were adjusted to suit the configuration of the Sentinel-2A/B wavebands and satellite geometric properties (i.e., Sun zenith angle, view zenith angle, relative azimuth angle). The shortwave bands (Band 11: centre wavelength 1610 nm and Band 12: centre wavelength 2190 nm), which are sensitive to vegetation variation and vegetation water-related indices (NDII, MSI, GVMI) generated from the Sentinel-2A/B data, were used as sources for LFMC estimation. To address the ill-posed inversion problem where different RTM input combinations may correspond to almost identical spectra, ecological rules were applied to regularize the RTMs, removing abnormal simulations and making the LFMC simulation scenario more realistic.

Live Fuel Moisture Content measurements from Globe-LFMC 2.0 (Yebra et al. 2024) for Australia were used to validate the LFMC estimates. Since the high resolution of Sentinel-2A/B (automatically resampled to 10 m for optical to shortwave bands by the GEE platform) may lead to mismatches between field measurement scale and satellite observation scale, LFMC measurements were filtered spatially and temporally according to the following rules: (1) At the spatial scale, LFMC values sampled from highly heterogeneous sites were removed using the coefficient of variation (CV), which was calculated as the ratio of the standard deviation to the mean Sentinel-2A/B NDVI within a 100 m square area centred on the target site (Eq. 11). Following Quan et al. (2024), LFMC data were considered valid for the experiment only when the CV at a given site was below 15%. (2) At the temporal scale, to enhance the stability of LFMC measurements and mitigate errors arising from various factors, outliers from multiple samples at the same site were filtered using the temporal rule proposed by Yebra et al. (2018) (Eq. 12). Additionally, LFMC sampled from different areas that are close to each other and belong to the same species were merged into a single value using their mean. With the measurements, the LFMC estimates achieved an accuracy of $R^2 = 0.63$, RMSE = 23.08%, $p < 0.01$ (see Appendix 1 Fig. A1).

$$CV = \frac{NDVI_{std}}{NDVI_{mean}} \times 100\% \tag{11}$$

$$\frac{LFMC_i - \mu}{\sigma} < x \tag{12}$$

where the *LFMCi* represents the *i*-th LFMC measurement in a series of continuous samples, μ denotes their mean, σ is their standard deviation, and x is the threshold value. Following the approach outlined by Quan et al. (2021), this study used $x = 2.1$ to identify and remove outliers.

2.4.4. Temporal Features of Selected Variables

In addition to estimation of LFMC and VIs for the peak drought time point in October 2023, we evaluated the temporal dynamics of selected LFMC and VIs. By following Yebra et al. (2018), the standardised difference (between 2019 and 2023) and change rate for the selected factors were calculated. The anomaly is represented by the z value as,

$$z = \frac{x - \mu}{\sigma} \tag{13}$$

where x represents the LFMC or VI value for October 2023, μ is the mean of the variable calculated for the reference period (October 2019 to October 2022), and σ is the standard deviation over the same period. The z-score characterizes how far a given observation deviates from its long-term mean in terms of standard deviation. Positive z-scores indicate conditions above the mean, while negative z-scores reflect values below the mean. These anomalies serve as indicators of vegetation stress or resilience, enabling the identification of regions experiencing unusual conditions. By capturing deviations from historical baselines, this approach highlights significant ecological disruptions and provides a robust framework for assessing canopy health.

To capture the temporal dynamics and assess the progression of canopy dieback, the change rate (CR) of each factor was calculated as:

$$\text{changerate} = \frac{x_{Sep.orAug.} - x_{October}}{x_{Sep.orAug.}} \times 100\% \qquad (14)$$

where $x_{\text{Sep or Aug}}$ represents the LFMC or VI value for September (one month before) or August (two months before) 2023, and x_{October} represents the corresponding value for October 2023. The CR quantifies the relative difference between consecutive observations, providing insights into the pace and magnitude of changes in LFMC and VIs over short temporal intervals. Rapid changes in LFMC or VIs may reflect acute stress events, such as drought or fire impacts, or recovery processes in post-stress conditions. By highlighting areas undergoing rapid transitions, the CR metric complements anomaly analysis, offering a more comprehensive understanding of canopy dynamics.

2.4.5. Supervised Classification of Canopy Dieback by Machine Learning

Random Forest models were built to diagnose spectral signatures of dieback stages, as well as to predict dieback stages across unclassified landscapes. The RF model is a strong classifier that combines multiple decision trees (weak classifiers) that can be applied to classification and regression (Breiman 2001).

Random Forest was implemented using MATLAB. The spatial extent of labelled polygons drawn using 3 m resolution PlanetScope imagery was trimmed to retain only areas fully covered by 10 m Sentinel grid cells. Spectral values for the 12 explanatory variables described above were extracted using all 10 m Sentinel grid cells fully covered by labels (manually classified polygons). Monthly-averaged Sentinel-2A/2B reflectance data were downloaded from the GEE platform and used to spatially classify the full extent of the case study area. Each decision classification tree was created by the training sample (70% of the explanatory variables) which was generated by the bootstrap aggregation algorithm. The validation sample (the remaining 30% of the explanatory variables) was used for model validation. The RF model was used to produce a prediction surface across the full extent of the study area (Fig. 3A) with classification of pixels to dead canopy, partially dead canopy, and live canopy, alongside other land cover types such as grassland and non-vegetation (bare ground) areas. These data were used to classify canopy dieback in October of 2023. The model was subsequently used to classify canopy dieback as a monthly time series from January 2019 to December 2023.

2.5. Factors Associated with the Spatial Pattern of Canopy Dieback

Factors potentially influencing spatial patterns of dieback considered in this study include a mix of abiotic and biotic variables and can be classified into three categories: (1) topography related variables including Northness, Topographic Wetness Index (TWI), and Topographic Position Index (TPI), (2) fire related variables including fire severity, whether burned or unburned, and whether burned by prescribed fire, and (3) land management variables including management zones, areas previously affected by BMAD, and presence of hardwood plantations (Fig. 4). Available climatic factors expected to be relevant to dieback (i.e., maximum temperatures, total rainfall, vapour pressure deficit) are too spatially coarse (~1 km) to be considered useful for prediction of fine-scale (10 m) dieback response. Therefore, they were not considered here. Authoritative data sources of spatial variables, as well as the links used for downloading, are provided in Appendix 1, Table A1. For the purposes of these analyses, the area under study was limited to public lands including protected areas and State Forests. The area was masked by Major Vegetation Group based on the National Vegetation Information System (NVIS) products (See Appendix 1, Table A1), with only Groups 1-4 (Rainforest and Vine Thickets, Eucalypt Tall Open Forest, Eucalypt Open Forest, Eucalypt Low Open Forest) included for analyses.

2.5.1. Topographic Factors

The effects of three factors, Northness, Topographic Wetness Index (TWI), and Topographic Position Index (TPI) on canopy dieback were analysed in the study area. Northness is particularly useful in terrain analysis for assessing slope orientation (aspect), solar radiation, and ecological patterns. Aspect is routinely correlated with vegetation responses; however, due to the circular nature of the data (0-360 degrees), for this study, aspect was transformed into 'Northness' (derived as sin(aspect * ∏ / 180)). Northness values range continuously from -1 (indicating a south-facing surface) to 1 (indicating a north-facing surface). The Topographic Wetness Index (TWI) quantifies the potential for water accumulation and soil moisture based on topographic features. This index is widely applied in hydrology, soil science, and environmental modelling. Values of TWI typically range from 4-20 with low values representing drier conditions, often associated with hilltops, ridges, and well-drained slopes, while higher values indicate wetter conditions, often found in gullies and depressions. The Topographic Position Index (TPI) measures the relative elevation of a point compared to the average elevation of its surrounding area. TPI values help classify terrain features: TPI > 0: indicates the area is higher than its surroundings (e.g., ridges, hilltops); TPI ≈ 0: indicates the point is at a similar elevation to its surroundings (e.g., flat areas); TPI < 0: indicates the point is lower than its surroundings (e.g., valleys, depressions). All three indices were calculated with QGIS software using the SAGA Next Gen tool with input from Digital Elevation Model (DEM) data.

2.5.2. Fire Related Factors

Fire severity and burned area here refers to fires during the 2019-2020 fire season. Several small fires were observed after 2020, but the extent and severity were negligible compared to the 2019-2020 fire season. Fire Extent and Severity Mapping (FESM) (NSW DCCEEW, 2020) was classified into four ordered categories: (1), “low (unburnt canopy)” (2), “moderate (partial canopy scorch)” (3), “high (complete canopy scorch)” (4), and “extreme (full canopy consumption)”. Burned area is a binary categorical variable (“burned” = 1, “unburned” = 0) included to simplify analyses by separating the effects of unburned area from the FESM categories.

2.5.3. *Land Management Related Factors*

Management zones were coded for analysis as categorical factors:

- conservedArea (0) protected areas including National Parks and Reserves as provided by the Collaborative Australian Protected Areas Database (CAPAD) but excluding State Forests areas managed for conservation;
- conservedForest (1) State Forest areas managed for conservation including Forest Management Zones 1-3B;
- harvestedForest (2) State Forest areas managed for harvest, Forest Management Zone 4.

Protected areas were split between State Forests managed for conservation and other protected areas, mainly National Parks and Reserves, so that land tenure and management could be evaluated as a predictor of canopy dieback severity.

Areas utilised for hardwood forestry plantations and areas exposed to prescribed burns between 2020 and 2023 were included as provided.

2.5.4. *Bell Miner Associated Dieback (BMAD) Related Factors*

Silver and Carnegie (2017) define BMAD as follows: “Bell miner associated dieback (BMAD) is a process where eucalypts enter a cycle of defoliation and regrowth, but if conditions persist, large areas of dieback and tree death can occur. While there are multiple causes of eucalypt forest dieback, this form is associated with an over-abundance of the native bell miner bird (*Manorina melanophrys*) and psyllid insects (including *Glycaspis* and *Cardiaspina* spp.).”

Estimates for areas previously impacted by BMAD (“nonBMADarea” = 0; “BMADarea” = 1) were based on aerial surveillance in 2015 and 2017 and were included as provided by NSW DPI Forestry.

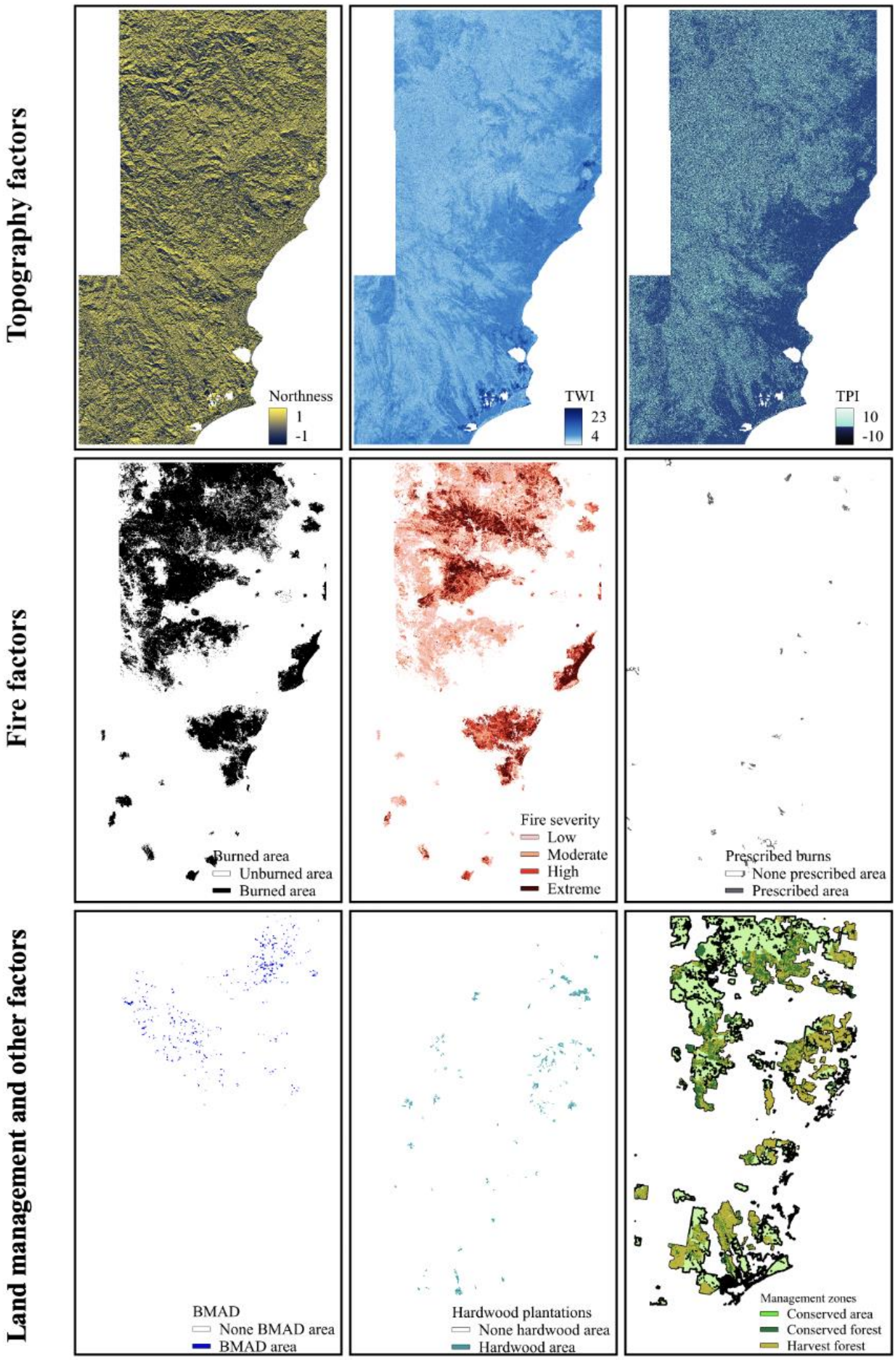

Figure 4. Spatial factors evaluated as predictors of canopy dieback severity observed in October 2023 on the NSW North Coast. Factors are grouped by topography, fire, land management and BMAD.

2.5.5. Combining LightGBM with SHAP Models for Analysis of Spatial Variables

Drought has been identified as the primary factor driving the 2023 canopy dieback event in the study area (see Fig. 1). To examine the influence of topography, fire, and land management factors in explaining spatial patterns of dieback observed across the study area, an additional machine learning approach, the Light Gradient Boosting Machine (LightGBM) model, was utilized. The LightGBM is a gradient boosting (GB) variant known for its efficiency in handling large, structured datasets with high training speed (Ke et al. 2017). As an ensemble learning method, GB combines multiple weak learners to create a robust predictive model, often achieving higher accuracy than single models (Che et al. 2011). LightGBM offers significant advantages over other machine learning models such as XGBoost and RF, particularly in its ability to handle null data, which RF cannot process effectively. In this study, the high-resolution Sentinel-2A/B data (10 m) generated an extremely large dataset, where LightGBM demonstrated superior efficiency, with lower memory consumption and faster computation times compared to RF and XGBoost. While all three models employ the ensemble learning paradigm, LightGBM often outperforms RF due to its sequential tree-building approach through boosting iterations, as opposed to RF's independent tree construction and output averaging (Breiman 2001; Che et al. 2011). We acknowledge the potential non-independence (multicollinearity) among predictor variables in our dataset, such as topographic metrics (e.g., aspect, TPI, TWI) and their possible relationships with land management or fire history. To assess multicollinearity, we examined pairwise correlations among predictors. Additionally, our modelling approach using LightGBM is inherently robust to multicollinearity in terms of predictive performance. Unlike linear models, LightGBM does not assume predictor independence and is able to identify the most informative features at each split without inflating variance due to correlated variables.

The LightGBM model was combined with Shapley Additive exPlanations (SHAP) to provide detailed analysis by quantifying the contributions and interrelationships of individual explanatory variables to the occurrence of dead and partially dead canopy events. SHAP is a widely used method for interpreting machine learning models, offering insights into how each feature impacts the model's predictions, thereby enhancing model transparency and interpretability (Lundberg 2017). SHAP calculates the contribution of each feature to the model's predictions based on cooperative game theory principles, where each feature is treated as a "player" contributing to the overall outcome. This approach not only clarifies which features drive the predictions but also illustrates how these features interact with each other, providing a deeper understanding of the model's decision-making process (Emaminejad et al. 2023). SHAP is more robust than standard feature attribution because (i) SHAP evaluates the contribution of a feature in the context of all other features, and (ii) even if two features are highly correlated, SHAP fairly distributes the importance between them across all permutations. SHAP values also offer a comprehensive breakdown of feature contributions for each individual prediction rather than an aggregate result, making it possible to explain model behaviour on a granular level. Thus, LightGBM and SHAP provides a robust framework for identifying key drivers of canopy dieback, even when full independence among predictors is not present.

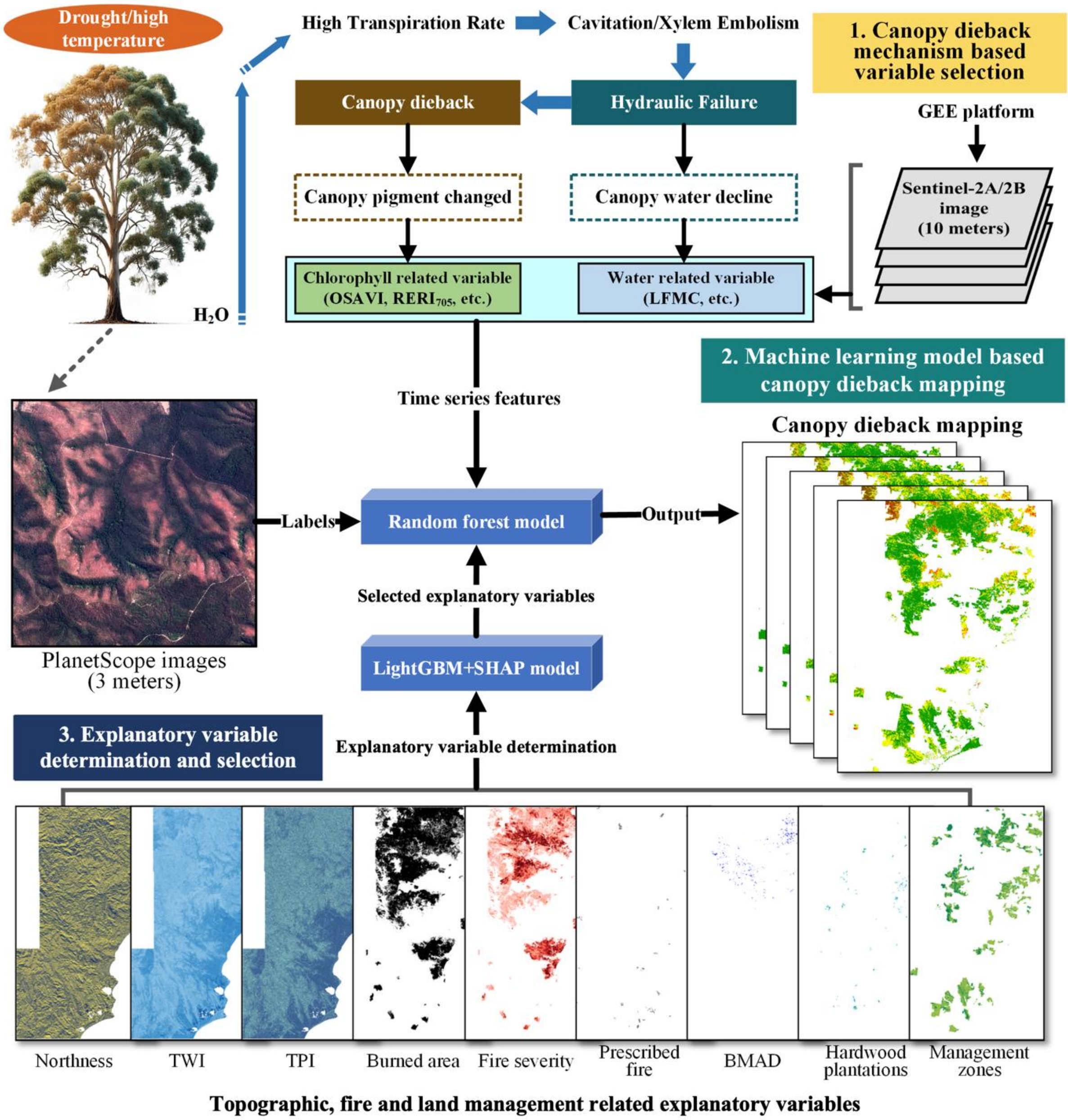

Fig. 5. Flowchart summarising the methodology for detection of canopy dieback and analysis of explanatory variables based on remotely sensed LFMC, greening indices, and environmental factors.

2.6. Validation

The performance of the canopy dieback detection method developed in this study was validated from two perspectives: (1) Performance of the RF model in classification of canopy dieback; (2) Field survey-based validation of canopy dieback.

The performance of the machine learning model was assessed based on the classification accuracy achieved by the RF algorithm. The accuracy of the RF model, derived from repeated runs, provided a reliable measure of its ability to distinguish between dead, partially dead, and live canopy conditions. This evaluation ensured the robustness and consistency of the machine learning approach.

The performance of the canopy dieback classification was further validated using a Confusion Matrix. The Confusion Matrix, a widely used tool in classification tasks, provides a comprehensive evaluation by comparing the predicted classifications (e.g., dead, partially dead, and live canopy) with the actual field observations. Specifically, several key performance metrics were derived to quantify the accuracy of the model:

- Overall Accuracy: The proportion of correctly classified samples out of all samples.
- Precision: The ratio of true positives to the total predicted positive cases, reflecting the model's ability to avoid false positives.
- Recall (Sensitivity): The ratio of true positives to the total actual positive cases, indicating the model's capacity to detect dieback conditions.
- F1 Score: A harmonic mean of precision and recall, providing a balanced evaluation of the model's performance.

These metrics enabled a detailed evaluation of the strengths and weaknesses of the model among different canopy conditions. The validation process highlights the overall effectiveness of the proposed method and areas where classification accuracy could be further optimized.

2.7. Ground-Based Observations of Canopy Condition and Tree Mortality

Ground survey sites were identified within AOI-1 to provide estimates of tree mortality and canopy condition in forest patches that sustained visible canopy dieback during the September-October 2023 period in comparison to patches that remained green through this period. Survey sites were selected during the manual labelling process, with plots distributed across terrain positions associated with varying degrees of canopy dieback (ridge, south-facing slopes, gullies). In all, 19 plots of 30 m diameter were established within Bulls Ground State Forest. In each plot, tree species was recorded and diameter at breast height over bark (DBH) was measured for each tree >10 cm DBH. Crown condition was assessed for each tree in each plot based on a canopy health score, which is derived from visual estimates of canopy density, canopy size, dead branches, epicormic growth and canopy browning (see Nolan et al. 2021 and Appendix 2 for detailed method description). Resprouting and regrowth (presence and position of epicormic resprouts) were documented in surviving trees along with the presence of significant injury to the main stem (e.g., fire scar or logging scar). Data collected were used to determine whether patches subject to canopy dieback in September-October 2023 had greater stem mortality (either topkill or complete tree mortality) and lower canopy health scores compared to patches that maintained a canopy with no evidence of dieback through this period. In this case ‘stem mortality’ refers to either ‘topkill’, which describes the death of all above ground biomass, or tree mortality, which refers to the death of the whole tree, with no possibility for basal resprouting to occur. Trees were classed as ‘dead’ in ground surveys, if they were shedding bark and showed no visible signs of recovery of live tissue above ground. However, it is not possible to confirm whole plant mortality without return visits to check for basal resprouting at a later date. Trees that had clearly died in years before the 2023 drought (no bark persisting, wood bleached of colour from long term UV exposure) were listed as ‘dead/ pre-drought’.

3. Results

3.1. Mapping of Canopy Dieback

3.1.1. Performance of Selected Vegetation Indices

To evaluate the relationship among variables and their utility in detection of canopy dieback, correlation analysis and feature importance rankings were performed (Fig. 6). The importance rankings were calculated as the average of 100 iterations of the RF model, with error bars indicating the standard deviations to reflect the robustness and reliability of the rankings. Feature importance rankings and a correlation matrix for spatial variables associated with canopy dieback are provided in Fig. 6 (a and b). Among the variables, LFMC had the highest importance for classifying canopy dieback severity, followed by the chlorophyll-related OSAVI and RERI705, although OSAVI was strongly correlated with LFMC (r = 0.80). The variable RERI705 was weakly correlated with other factors, highlighting its potential to provide some additional independent information for classification of canopy dieback severity. Therefore, LFMC and RERI705 were retained while other variables with high mutual correlations were excluded from further analysis to avoid redundancy and multicollinearity.

The feature importance rankings of these selected variables (LFMC and RERI705) and their temporal dynamics, including anomaly and CRs, were further evaluated (Fig. 6c and d). The most influential factor remained LFMC. The temporal features of the selected variables, particularly anomaly and CRs, also showed high importance.

3.1.2. Supervised Classification of Canopy Status by Machine Learning

Based on the selected LFMC, RERI705, and their temporal features derived from Sentinel-2A/B imagery at a spatial resolution of 10 m, canopy dieback classification was performed for October 2023 across the full extent of the study area (Fig. 7). The classification utilized the RF model with an overall accuracy of 0.94. The map delineates areas of dead canopy (red), partially dead canopy (yellow), and live canopy (green), as well as other land cover types, including grassland (light green) and non-vegetation areas (brown). The high-resolution imagery in the centre column and the corresponding classified maps in the right column depict three representative areas within the study area (Fig. 7). Statistics describing the area of each canopy dieback class within spatial variable categories are provided in Appendix 3 (Table A2-A9).

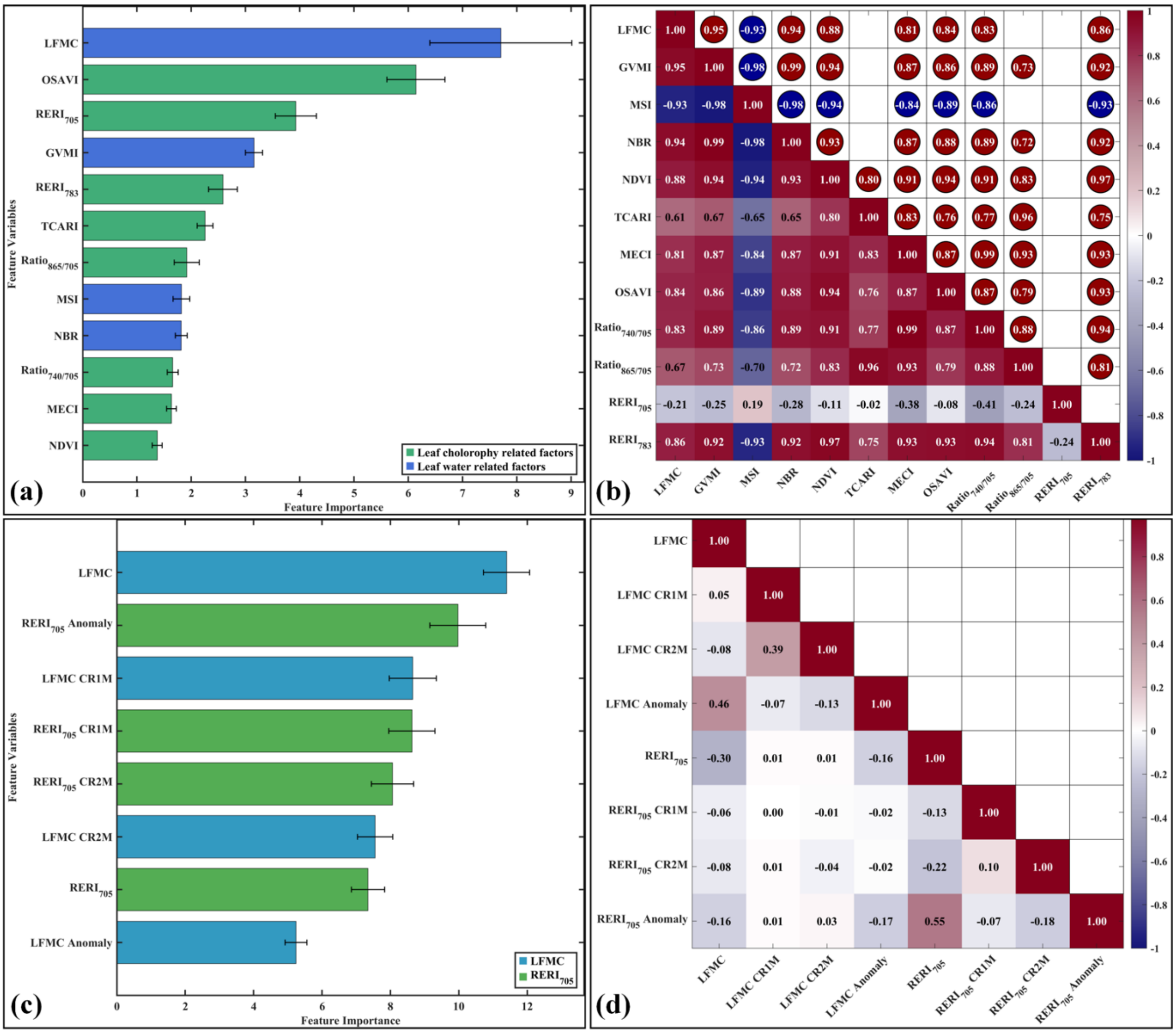

Figure 6. Importance rankings for selected variables and indices related to classification of canopy dieback severity. Panels (a) and (b) show the importance rankings and correlation matrix for the selected water and chlorophyll related variables. In the correlation matrix, correlation coefficients are shown above and below the 1:1 line, with only significant relationships shown above the line. Panels (c) and (d) present the importance rankings and correlation matrix for the filtered features (LFMC and RERI705), and their temporal characteristics, including Anomaly and change rate (CR). The importance values are averaged over 100 iterations of the Random Forest model, with error bars representing standard deviation.

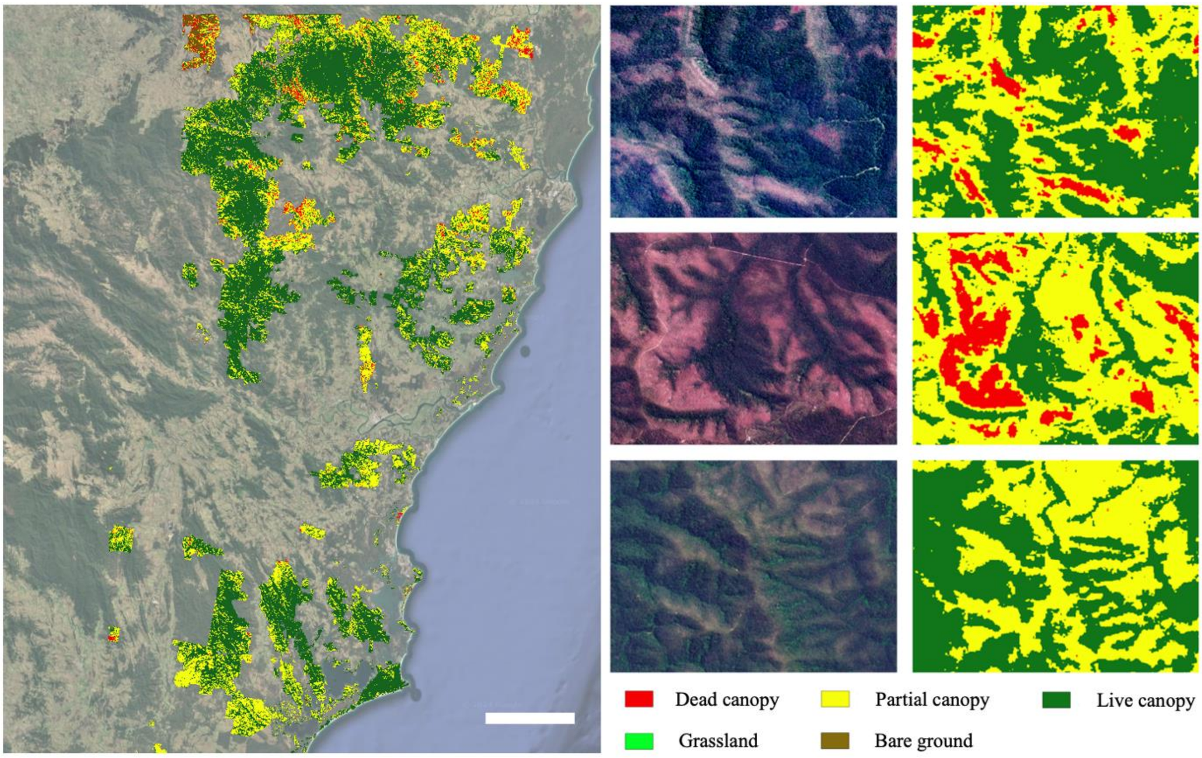

Figure 7. Canopy dieback severity mapping for the study area using the selected LFMC, $RERI_{705}$, and their temporal features derived from Sentinel-2A/B imagery at a spatial resolution of 10 m and Random Forest model. The classification highlights areas of dead canopy (red), partially dead canopy (yellow), and live canopy (green), alongside other land cover types such as grassland (light green) and non-vegetation areas (brown). The area shown has been clipped to public lands including National Parks, Nature Reserves, and State Forests. The right column displays the classified maps for three representative areas, corresponding to the high-resolution imagery in the centre column. The scale bar represents 20 km.

3.2. Analysis of Variables Associated with Spatial Patterns of Canopy Dieback

The correlations among variables related to topography, fire, and land management are shown in Fig. 8. The burned/unburned area and fire severity exhibited a strong correlation (r = 0.90), while the correlations among other variables were not significant (Fig. 8a). As expected, some topographic variables were related, with a correlation between TPI and TWI (r = 0.49). Other variables showed no meaningful correlation, e.g. fire severity showed no meaningful correlation with Northness (r = 0.05) or TWI (r = –0.10), so these were considered as independent in effect. While LightGBM does not assume independence among predictors, and SHAP values help interpret feature influence even under multicollinearity, we interpret identified variable effects as associative, not strictly causal. The results reflect joint contributions of predictors in the model and warrant further targeted analyses (e.g., stratified by topography) to disentangle the unique effects of land management or fire history.

Based on the LightGBM and SHAP model, Northness emerged as the most influential predictor for both dead and partial dead canopy conditions, followed by TPI and fire severity (Fig. 8 b, c, and d). Management zones and TWI showed moderate importance, and prescribed burns, BMAD, and hardwood plantations showed very low importance. For dead canopy, topographic factors, particularly Northness and TPI, contributed the majority (65.0%) of the predictive importance, followed by fire-related factors such as fire severity (22.7%). Land management factors, including prescribed burns and management zones, accounted for a smaller share (12.3%). Similarly, for partially dead canopy, topographic factors remained the primary contributors (69.8%), followed by fire-related (16.3%) and land management factors (13.8%).

Although prescribed burns, BMAD, and hardwood plantations exhibited a very low importance rank overall (Fig. 8b), this does not imply that they are not important for detecting canopy dieback. As illustrated in Fig. 9, which highlights the most influential factors at the spatial pixel scale, these three factors often emerge as the top contributor in areas where they were present (Fig. 9). Their low overall importance rank is primarily due to their limited spatial extent (Fig. 4). Similarly, high and extreme fire severity emerged as the primary driving factor behind canopy dieback in the affected regions. Outside areas that were severely burnt during the 2019-2020 fires, topographic factors, particularly Northness and TPI, exhibited the highest influence on canopy dieback.

For both dead and partially dead canopy, Northness, TPI, fire severity, hardwood plantations, and BMAD exhibited clear effects on canopy dieback (Fig. 10). Specifically, canopy dieback (both dead and partially dead) was more likely to occur in areas with north facing aspect, ridges, high to extreme fire severity, outside of hardwood plantations, and in areas mapped as BMAD. Topographic wetness index, prescribed burns, and management zones also exerted some influence on canopy dieback class although their effects were not as clear. For dead canopy, lower TWI values (indicating drier positions in the landscape), areas subject to prescribed burns, and conserved areas (National Parks, Reserves) were associated with an increased likelihood of canopy dieback. A higher likelihood of partially dead canopy was associated with prescribed burns, and conserved forest (State Forests managed for conservation). The effects of burned/unburned area on dead canopy and TWI on partially dead canopy were ambiguous, showing no clear positive or negative influence. This suggests that these factors are interrelated with others, complicating their independent effects. For example, as illustrated in Fig. A2 (see Appendix 1), the effect of TWI on partially dead canopy is influenced by fire severity, management zones, and Northness. This indicates that partial canopy dieback may also occur in areas with high to extreme fire severity, harvested forest zones, and north-facing regions, even under high TWI values (indicative of wetter terrain position).

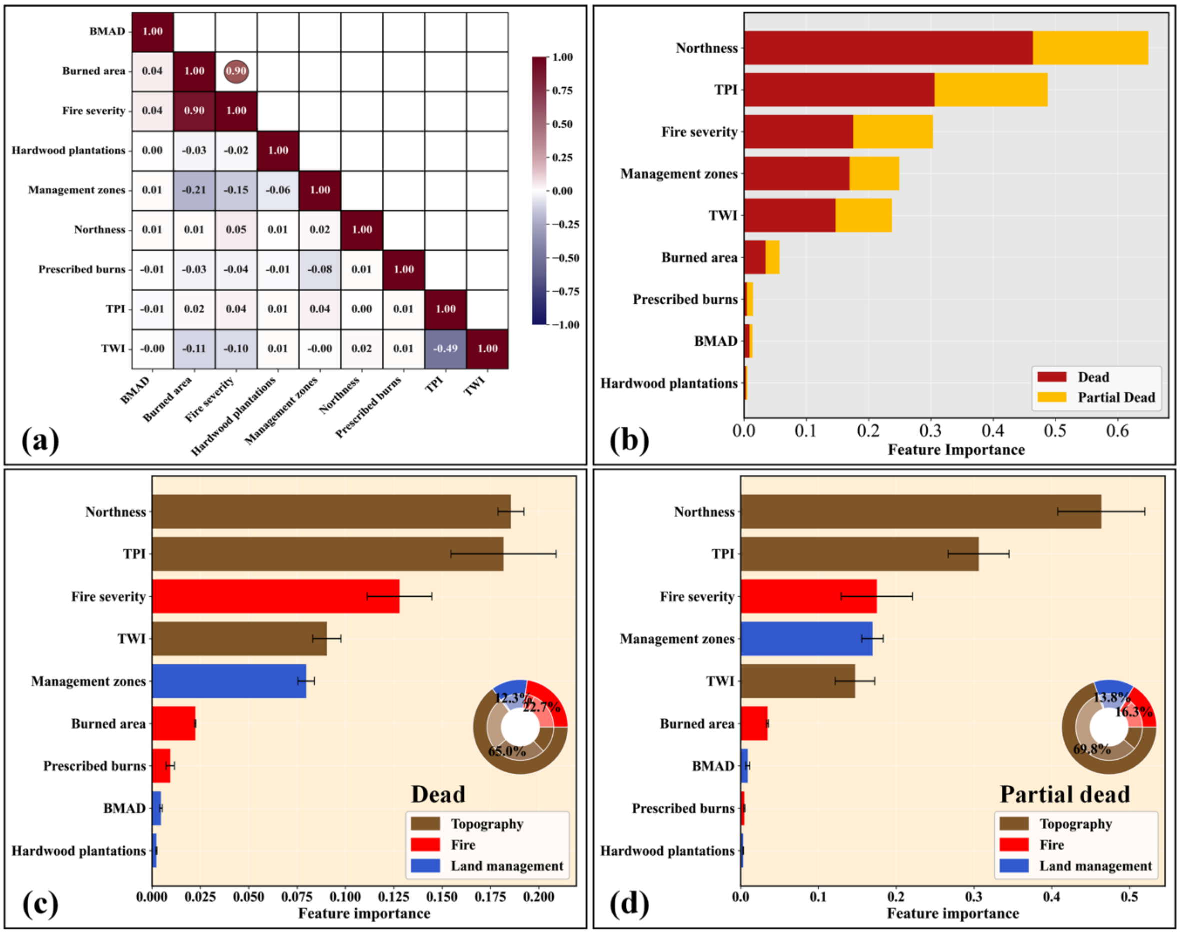

Fig. 8 (a) Correlation among topography, fire, and land management related variables. (b) the total importance rank of these features for prediction of dead (c) and partially dead (d) canopy classes. The overall feature importance rankings are based on 100 iterations of the LightGBM model, with error bars representing standard deviation.

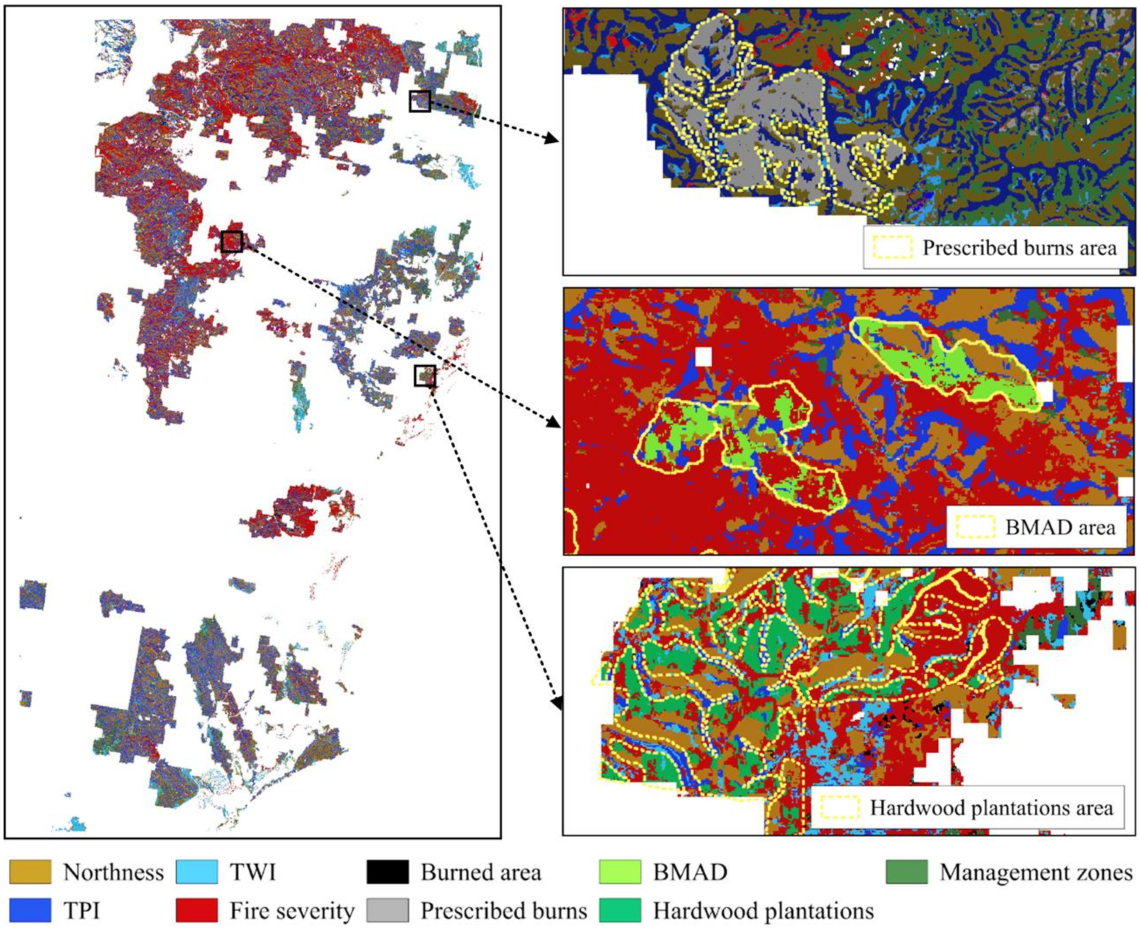

Fig. 9. The most important variable associated with dead and partially dead canopy for individual pixels, with enlarged sections showing areas in which prescribed burn, BMAD and hardwood plantation variables showed the greatest effects.

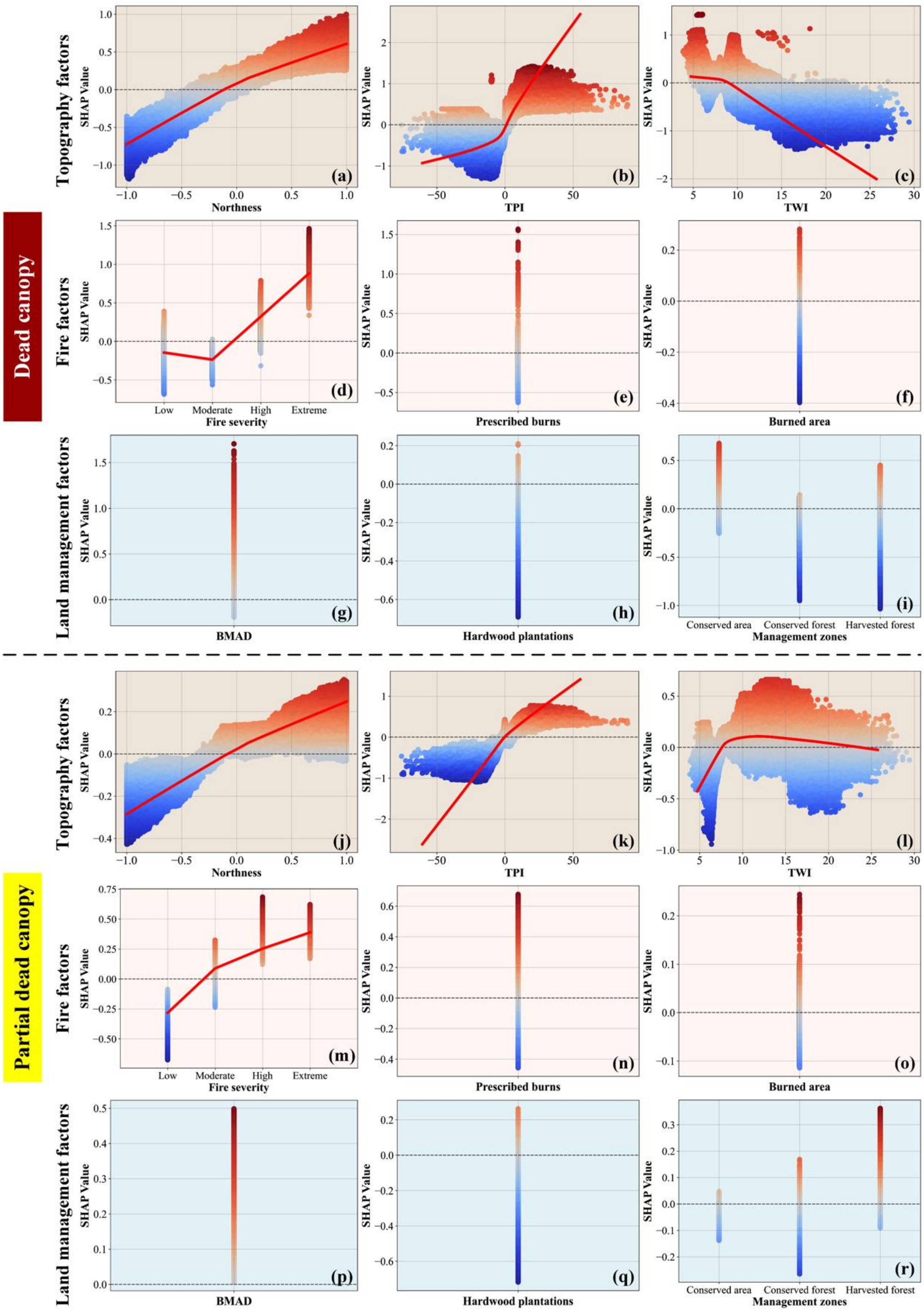

Fig. 10: SHAP plots illustrating the relationship between topographic, fire, and land management variables with canopy dieback class. (a)-(i) show the interactions for dead canopy, and (j)-(r) for partially dead canopy. Each panel represents the influence of different variable on SHAP values, with colour gradients indicating the strength of contribution of each variable.

3.3. Performance Comparison and Time-Series Canopy Dieback Mapping

When considering the features LFMC, RERI705, and topographic factors (Northness and TPI), the accuracy of canopy dieback classification using the RF model increased from 0.94 to 0.96 (Table 2). Among these factors, LFMC had the highest feature importance, followed by RERI705 Anomaly, Northness, and TPI (Fig. 11). Combining LFMC and RERI705 increased the model's F1-Score to 0.89 (Table 2). When environmental factors were included alongside these indices, the F1-Score was 0.91, with an overall improvement in accuracy, precision, and recall metrics.

Table 2 Accuracy of different selected variables for prediction of canopy dieback.

Factors	Overall Accuracy	Precision	Recall	F1-Score
LFMC	0.92	0.87	0.82	0.84
$RERI_{705}$	0.83	0.76	0.65	0.69
LFMC+ $RERI_{705}$	0.94	0.91	0.87	0.89
Topography factors	0.84	0.51	0.37	0.41
All	0.96	0.93	0.90	0.91

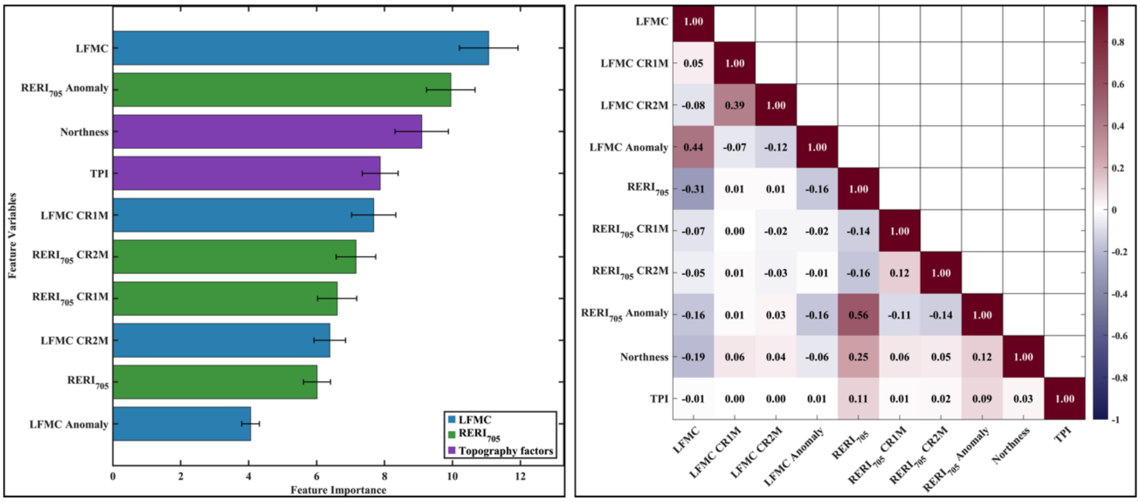

Fig. 11. The importance rankings and correlation matrix for the selected LFMC, RERI705, and environmental factors.

Monthly-averaged Sentinel-2A/2B reflectance data from the GEE platform were analysed to classify canopy dieback from January 2019 to December 2023 (Fig. 12). Peaks in partial canopy dieback area were observed in November 2019, and October 2023, with a smaller peak in October 2021. Extensive canopy dieback was detected in December 2019, corresponding to significant increases in both partial and complete dieback areas. The increase in partially dead canopy beginning in June 2019 can be attributed to drought stress. The sharp increase in dead canopy can be attributed to the Black Summer fires (Fig.12B, Fire severity), rather than drought-induced canopy dieback. Spatial distributions of canopy dieback during these periods are shown in the lower panel of Fig. 12, illustrating the affected regions over time.

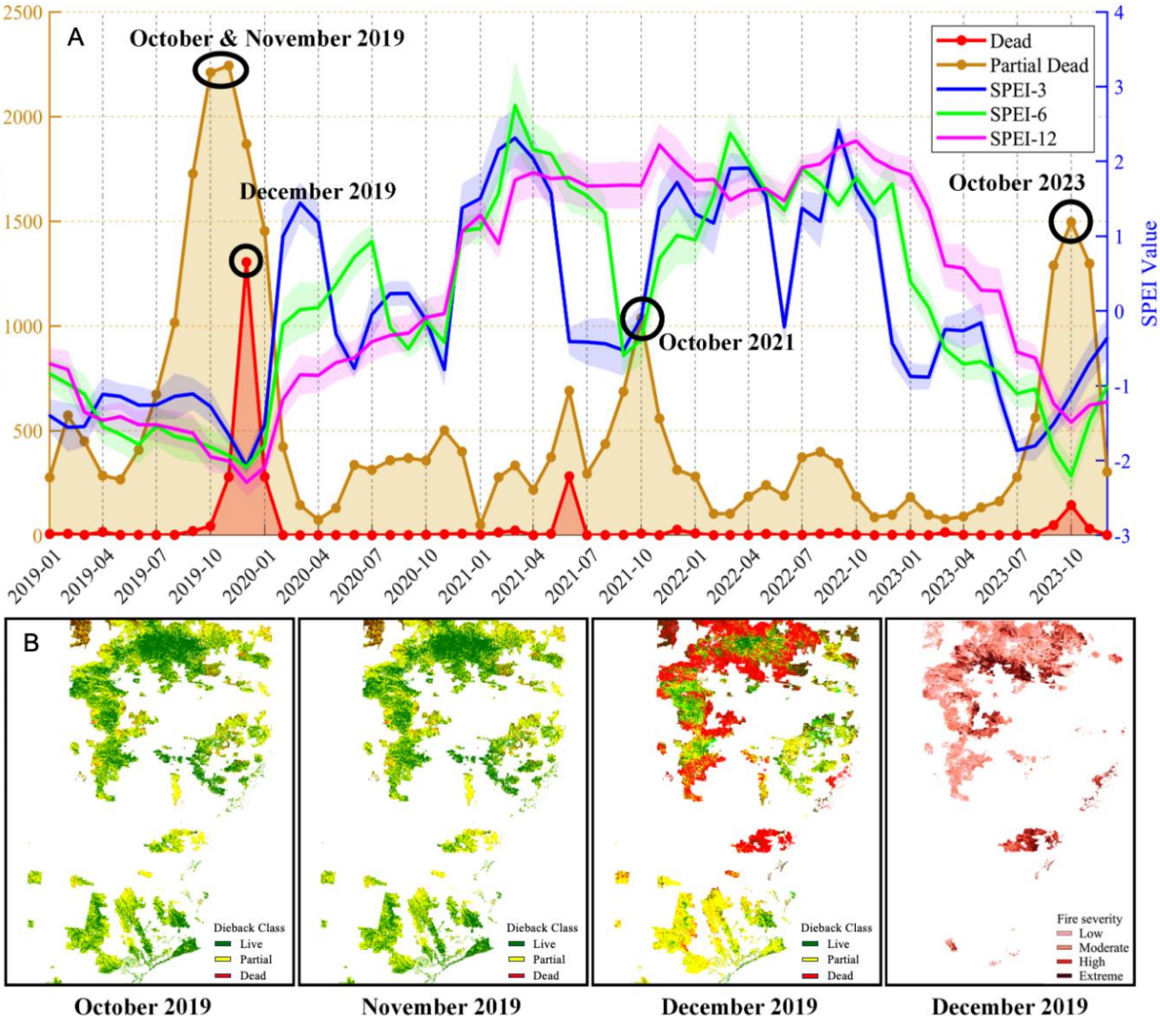

Fig. 12. Time-series and spatial mapping of canopy dieback for the study area. (A) Change in area (km^2) of dead canopy and partial dead canopy between January 2019 and December 2023. The Standardized Precipitation Evapotranspiration Index (SPEI) calculated for 3-, 6- and 12-month periods is shown overlaying the change in canopy dieback areas. (B) Spatial variation is canopy dieback classes shown for three different months covering the period of the Black Summer drought and bushfires and subsequent recovery and fire extent and severity map (FESM) for the study area.

3.4. Ground Based Observations

Ground based plot surveys were designed to provide insight into the longer-term impacts of canopy dieback on tree mortality and canopy condition. These surveys were conducted in September of 2024, approximately one year after the sudden canopy dieback event of 2023. Analysis of the data revealed that plots differed in the number of dead trees as a function of terrain type (ridge, gully or south-facing slope) with ridge plots having significantly greater proportion of basal area accounted for by dead trees compared to gully plots (Fig. 13). Plots that were classified as dead canopy by the RF model in October 2023 also had a significantly greater proportion of dead basal area. These results were mirrored in the assessment of canopy condition, with ridge plots having significantly lower canopy health score for surviving trees compared with gully and south-facing slope sites. These results indicate a possible legacy effect from the canopy dieback event in 2023, with a high proportion of dead trees and lower canopy health scores in plots that had experienced full canopy dieback. Plots classified as having partial canopy dieback also carried a higher proportion of dead basal area and had lower canopy health scores than sites classified as alive.

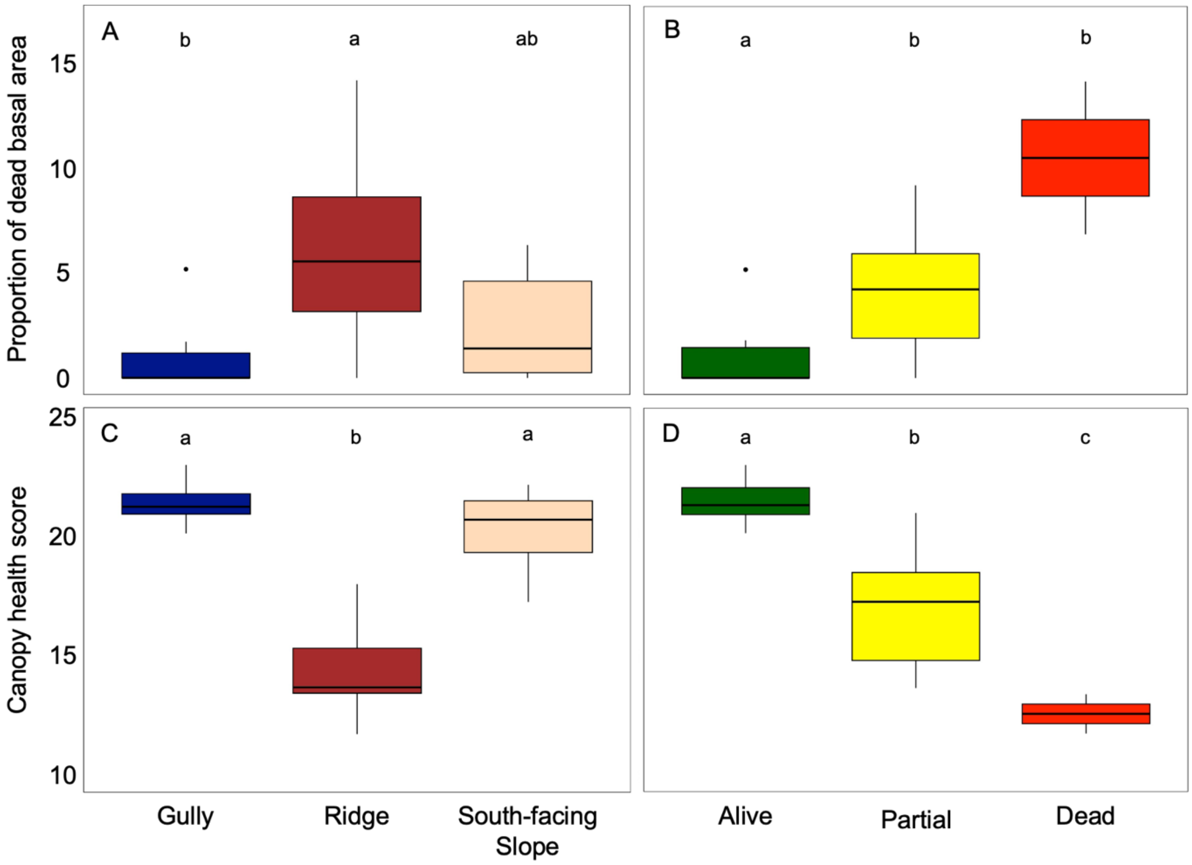

Fig. 13. Box plots showing (A) proportion of basal area accounted for by dead trees as a function of terrain position, and (B) canopy dieback class assigned by the Random Forest (RF) model for October 2023. (C) Mean canopy health score for plots as a function of terrain position, and (D) canopy dieback class assigned by the RF model for October 2023. Letters indicate significant differences at $p = 0.05$.

4. Findings, Recommendations, and Future Applications

4.1. Outcomes of Pilot Study

4.1.1. Identification of Canopy Dieback Using PlanetScope Imagery

PlanetScope imagery proved to be an effective tool for detailed canopy dieback assessment at a localized scale. The PlanetScope image library provides 3 m imagery from 2016 to present in the NSW coastal regions, allowing for investigation of canopy dieback over a significant time period that includes a severe drought (2017-2020), extensive bushfires (2019-2020) and an early season drought in 2023. The visual (3-band) imagery was ideal for manual identification of canopy dieback classes (dead, partial, live) over smaller areas (e.g., 1,000-2,000 km^2) and shorter timeframes using three standard Education and Research licences from PlanetScope, which each provide 5,000 km^2 of downloaded imagery per month. The near-daily return interval of PlanetScope imagery was particularly valuable in capturing the peak expression of dieback, rather than relying on longer temporal composites that may obscure transient canopy stress. Disadvantages of PlanetScope relative to other satellite remote sensing platforms include limited spectral bands (4 bands versus 13 bands for Sentinel-2), lack of systematic atmospheric corrections, and higher costs if larger areas are to be mapped. PlanetScope and Sentinel-2 have geolocation errors of less than 10 m and less than 12 m, respectively, meaning the imagery cannot be used to track individual tree crowns over time without corrections with high precision ground data. However, both systems provide ample resolution to identify the large and small patches of canopy dieback that are typically observed during environmental stress events.

4.1.2. Regional Mapping of Canopy Dieback Using Machine Learning

A supervised classification approach, leveraging RF and Sentinel-2 imagery, allowed for the extrapolation of manual canopy dieback classifications from higher resolution PlanetScope imagery across the broader study area of public lands in the NSW North Coast. The use of machine learning aligns with successful applications in fire severity mapping, such as Gibson et al. (2020) in a study using Sentinel-2 imagery to classify burn severity in southeastern Australia. The approach underlying the Fire Extent and Severity Mapping (FESM) product showed that spectral indices sensitive to vegetation moisture and structure can effectively differentiate burn severity levels. In our study, the combination of live fuel moisture content (LFMC), vegetation indices, and spatial features significantly improved classification accuracy, achieving an overall accuracy of 94–96% against training data generated from PlanetScope imagery. The model effectively delineated areas of dead, partially dead, and live canopy, demonstrating the feasibility of machine learning-based mapping for drought-induced canopy dieback. The study highlights the potential for integrating machine learning with freely available remote sensing data to enable regional and smaller scale dieback assessment.

Some areas of overprediction (overestimate of canopy dieback) were identified, particularly where tree canopy cover was lower than in the AOIs in which training data were generated from PlanetScope imagery. An example of this was found in the northwestern corner of the study area, in which low hills contained within Oxley Wild Rivers National Park were classified as bare ground or dead canopy. In areas with low canopy fraction such as this, it is assumed that the grass understorey browns quickly in response to drought, producing signals associated with severe canopy dieback. This issue may be addressed by generation of further training data targeted at woodlands with sparse tree canopy layers combined with targeted collection of ground truthing data and use of LiDAR to measure changes in vegetation structure.

4.1.3. Evaluation of Variable Associated with Spatial Patterns of Canopy Dieback

Our approach, combining the machine learning model LightGBM and SHAP values, provides a robust framework for assessing variable importance. However, it is important to note that these analyses were designed to identify robust predictors of canopy dieback rather than make strict causal inferences.

Analysis of topographic, fire history, and land management variables revealed distinct spatial patterns of canopy dieback. Northness and Topographic Position Index (TPI) emerged as the strongest predictors, with dieback more pronounced on north-facing slopes and ridges. Fire severity from the 2019-2020 Black Summer bushfires also contributed to spatial variation in canopy loss, while management variables, such as forestry operations and conservation status, had a moderate influence.

Analysis of SHAP values (Fig. 10) highlighted the substantive role of topographic variables Northness, TPI, and TWI in determining canopy dieback severity. TPI, which describes relative landscape position, revealed that ridges and exposed upper slopes (high positive TPI values) had a greater likelihood of dead canopy. These areas are more likely to have higher solar radiation, greater evaporative demand, and reduced soil moisture retention, all of which amplify drought stress (Inbar et al. 2018; Metzen et al 2019). Conversely, low TPI values (gullies and lower slopes) were associated with lower probability of canopy dieback, likely due to sheltered microclimates and greater retention of soil water during drought. Similarly, TWI, which quantifies potential terrain-controlled soil moisture accumulation, indicated that areas with low TWI values (well-drained, drier sites) were more likely to exhibit dead canopy. Areas with higher TWI values (better soil moisture retention) had a greater proportion of partially dead canopy, although this was due to interaction with other variables including Northness and fire severity. For example, areas with high TWI values were most likely to have partial dieback if they were north facing or had been severely burned in 2019. Northness, which measures solar exposure based on aspect, was the most important variable related to canopy dieback patterns. North-facing slopes (values near 1), which receive greater solar radiation, were strongly associated with dead canopy, whereas south-facing slopes (values near -1) exhibited less canopy dieback and tree mortality, likely due to reduced exposure to heat stress and/or improved soil moisture conservation.

The importance of aspect and topographic position could also be linked to shallower, rockier soils on ridges compared with gullies and south facing slopes. Previous work in forests of southeastern Australia indicates the soils on ridges are generally shallower, meaning that trees do not have access to deeper soil layers and the more persistent access to soil water they provide (Inbar et al. 2018; Metzen et al. 2019). These studies also indicate that southward facing slopes have deeper soils than north facing slopes, with the rate at which soil depth increased from the ridge to gully being higher on south facing slopes (Inbar et al. 2018). This suggests that ridges and north facing slopes dry faster during drought conditions and the onset of severe water stress would occur earlier than in adjacent gullies and south facing slopes. It is likely that this would lead to compounding effects and negative feedback over time, with sparser vegetation contributing less to soil development relative to gullies and south facing slopes. This would be exacerbated by higher tree mortality caused by cyclic disturbance events.

Partial and full canopy dieback were also more likely in areas that were classified as high or extreme burn severity during the 2019-2020 bushfire season. On a pixel basis, fire severity was generally the most important factor in areas severely impacted in the 2019-2020 fires, e.g., Mount Bass State Forest, Werrikimbe National Park (Fig. 9). The higher likelihood of canopy dieback in areas previously impacted by fire suggests a potential legacy effect from the 2019/2020 bushfires. The stronger response to drought in these areas may be driven by (i) loss of canopy trees leading to altered microclimates, with the regenerating understorey browning off more quickly than tree canopies, (ii) recovering trees with a high proportion of epicormic growth that is more sensitive to drought stress. However, the possibility of synergistic effects between pre-existing dryness, fire severity, and drought stress is also acknowledged; for example, areas that were drier prior to the 2019/2020 fires may have experienced both higher fire severity and a greater susceptibility to dieback during the 2023 drought. While our data-driven approach (LightGBM + SHAP) identifies robust predictive associations, it does not directly incorporate mechanistic processes or disentangle complex temporal interactions among drivers. We therefore interpret these results as indicative of a potential legacy effect but not definitive evidence of causality. Further investigation, particularly stratified analyses and ground observations, are required to assess whether fire and drought impacts exhibit a compounding or synergistic influence on long-term canopy health.

Variables relating to management and land tenure (management zones) were of moderate importance (Fig. 8), although the nature of the relationship varied between dead and partial canopy dieback classes (Fig. 10). National Park estates (conserved) were more likely to suffer full canopy dieback compared with State Forests managed for conservation (conserved forest) or areas of State Forest managed for harvest (harvested forest). The higher likelihood of finding dead canopy within National Park estates in the North Coast region may relate to the prevalence of high severity fires during 2019-2020 in some parks, with potential legacy effects noted above. In contrast, forests managed for harvest had the lowest predicted probability of dead canopy. However, for partial dieback, forest managed for harvest exhibited the highest positive SHAP values, indicating that, while they were less likely to experience full canopy dieback, they were more prone to intermediate levels of canopy dieback. Conserved (National Parks) and conserved forest (State Forest managed for conservation) had neutral associations with partial dieback, suggesting either greater stability or more binary responses to drought (i.e., survival or full mortality rather than intermediate stress levels).

Areas under plantation for hardwoods had a neutral to slightly negative association with dead and partial canopy dieback classes, implying that full canopy loss was less common in these managed forests compared to native, unmanaged stands. The higher SHAP values for partial dieback suggest that trees in these areas were more likely to experience moderate canopy decline rather than full canopy death.

Although BMAD was of low overall importance compared with other factors (Fig. 8c, d), the variable importance rankings are weighted by area effects, meaning that variables covering a smaller area were ranked of lower importance. As such, this result does not indicate that these variables are unimportant at smaller scales, as illustrated in Fig. 9, which shows the most important variable to dead and partial dead canopy classes at the scale of individual pixels. This indicates that BMAD was often the most important variable inside patches that had been identified as BMAD dieback affected by aerial surveillance from 2015 to 2017. The increased probability of full and partial canopy dieback associated with this variable suggests a putative legacy effect from previous dieback events.

4.1.4. Temporal and Spatial Variation in Canopy Dieback Classes Between 2019-2023

The methodology developed to evaluate canopy dieback in 2023 was applied to the time period between 2019-2023 to produce monthly mosaics of canopy dieback. Time-series analysis of Sentinel-2 imagery with supervised classification from the RF model revealed multiple episodes of canopy dieback, with major peaks in late 2019 (associated with the Black Summer fires) and late 2023 (linked to early-season drought). Analysis of SPEI values for the same period showed that peak dieback for dead and partial canopy classes coincides with timepoints at which SPEI reaches its most negative values. In 2019, widespread partial canopy dieback resulted from drought, while the fires caused a rapid increase in full canopy dieback in November and December of 2019. A smaller peak of partial dieback occurred in October 2021 and coincided with a short period of low SPEI values, although neither the intensity nor the duration of drought conditions was as great as in 2023.

Recovery in canopy greenness, as indicated by a decline in total area of dead and partially dead canopy classes, was rapid after major rainfall events and coincided with increasing SPEI values. This result suggests that almost complete recovery of the canopy occurs rapidly after the onset of rains, which is consistent with some other studies utilising remote sensing to evaluate the impacts of drought and fire in southeastern Australia (Byrne et al. 2021; Qin et al. 2022). However, recovery in spectral values is not necessarily representative of recovery of tree canopies but may instead represent growth of understorey beneath dead or defoliated trees (Bendall et al. 2023). This is supported by ground-based observations, which suggest legacy effects after severe droughts and fires (Matusick et al. 2018; Losso et al. 2022; Bendall et al. 2023). In this study, ground based observations showed that plots with dead canopy carried significantly more dead trees than those classified as partial or live (Fig. 13). This provides evidence that the rapid recovery in spectral values observed in remote sensing data do not capture the ongoing impacts of major disturbance events on trees.

4.1.5. Ground Based Survey Results

Ground-based surveys were done to assess longer-term impacts of canopy dieback on tree health. Field plots established within areas identified as having significant canopy dieback in 2023 revealed a strong correlation between remote sensing classifications and actual tree mortality rates, one year after the release from drought conditions. In patches that were classified as dead canopy by the RF model, it is assumed that the majority of trees experienced full canopy dieback. The ground-based observations indicate that trees accounting for 10% of basal area in these plots suffered whole tree mortality, while other trees were presumably able to recover canopy through a combination of epicormic resprouting and renewed growth from apical meristems. This is consistent with findings from studies examining drought induced mortality in eucalypt woodlands in other areas of NSW after the 2017-2019 drought, although other sites experienced greater loss of basal area through mortality or topkill after the drought

(Nolan et al. 2021; Losso et al. 2022). In this case, the effects of the October 2023 drought were apparent one year after the event, as indicated by the lower canopy health scores and the higher proportion of dead trees within plots classified as dead canopy.

Surveyed plots on ridge-top positions exhibited the highest proportion of dead basal area, consistent with predictions from the machine learning models indicating greater dieback in drier, more exposed landscapes. In contrast, gully and south-facing slope plots showed lower mortality rates and better canopy recovery. Trees within areas classified as dead canopy by the RF model also exhibited lower canopy health, suggesting a higher likelihood of long-term structural change in these forests. These findings underscore the importance of incorporating ground-based monitoring alongside remote sensing approaches to improve the accuracy of dieback assessments and better understand the ecological consequences of canopy loss. Future studies should expand ground surveys across a wider range of forest types and environmental conditions to refine predictive models and assess recovery trajectories over time.

4.2. Recommendations and Future Applications

4.2.1. Expand Regional Mapping Efforts and Training Data

- Given the success of this study in classifying canopy dieback using freely available Sentinel-2 data, a broader application of this methodology is recommended to assess dieback across other areas of NSW impacted by major stress events.

- Additional training data generated from high resolution imagery and ground truthing may improve the accuracy of canopy dieback mapping in vegetation types with lower canopy density.

4.2.2. Model Design and Interpretability

- Incorporation of plant community type (PCT) mapping and other vegetation mapping classification as additional training data may improve prediction outcomes from the Random Forest model across regions.

- Inclusion of multi-seasonal training data in the Random Forest model used for supervised classification of canopy dieback. This may improve model performance across seasons.

- Analyses with machine learning model LightGBM and SHAP values were designed to identify robust predictors of canopy dieback rather than make strict causal inferences. The results warrant further targeted analyses (e.g., stratified by topography) to disentangle the unique effects of other variables such as land management or fire history.

4.2.3. Monitoring of Individual Tree Crowns

- Investigate methods to help segment individual tree crowns from remotely sensed data products with a view to improving the accuracy of remote canopy dieback monitoring.

- Test potential for use of LiDAR data to automate crown segmentation, e.g., using available R packages such as lidR (Roussel et al., 2020); crown polygons overlaying high resolution RGB or hyperspectral imagery to allow rapid labelling canopy condition for individual tree crowns.

- Evaluate crown segmentation using very high resolution imagery (10-50 cm / pixel) to facilitate monitoring of canopy health in eucalypt dominated vegetation; would require data collection before, during, and after stress events.

4.2.4. Enhance Ground-Based Monitoring

- Incorporate more detailed, site scale forest management data into methods, including Coastal IFOA exclusions, tree retention areas, hazard reduction burns, time since previous harvest and other management activities.

- Establishing permanent ground survey plots across varying terrain positions and forest types will facilitate long-term validation of remote sensing-based dieback assessments.

- Regular tree health assessments, including hydraulic function measurements, could improve early detection of drought-induced stress.

5. References

Allen, C. D., Macalady, A. K., Chenchouni, H., Bachelet, D., McDowell, N., Vennetier, M., Kitzberger, T., Rigling, A., Breshears, D. D., Hogg, E. T., & Gonzalez, P. (2010). A global overview of drought and heat-induced tree mortality reveals emerging climate change risks for forests. *Forest Ecology and Management*, *259*(4), 660–684.

Atlas of Living Australia. (2024). *The dead tree detective*.

Bendall, E. R., Bedward, M., Boer, M., Clarke, H., Collins, L., Leigh, A., & Bradstock, R. A. (2022). Changes in the resilience of resprouting juvenile tree populations in temperate forests due to coupled severe drought and fire. *Plant Ecology, 223*(7), 907–923.

Bendall, E. R., Collins, L. C., Milner, K. V., Bedward, M., Boer, M. M., Choat, B., ... & Nolan, R. H. (2024). Demographic change and loss of big trees in resprouting eucalypt forests exposed to megadisturbance. *Global Ecology and Biogeography, e13842*.

Boer, M. M., Resco de Dios, V., & Bradstock, R. A. (2020). Unprecedented burn area of Australian mega forest fires. *Nature Climate Change, 10*(3), 171–172.

Breiman, L. (2001). Random forests. *Machine Learning, 45*, 5–32.

Bryant, C., Ball, M. C., Borevitz, J., Brookhouse, M. T., Carle, H., Cunningham, P., ... & Bothwell, H. (2024). Elevation-dependent patterns of borer-mediated snow-gum dieback are associated with subspecies' trait differences and environmental variation. *Austral Ecology, 49*(3), e13508.

Byrne, B., Liu, J., Lee, M., Yin, Y., Bowman, K. W., Miyazaki, K., ... & Paton-Walsh, C. (2021). The carbon cycle of southeast Australia during 2019–2020: Drought, fires, and subsequent recovery. *AGU Advances*, *2*(4), e2021AV000469.

Che, D., Liu, Q., Rasheed, K., & Tao, X. (2011). Decision tree and ensemble learning algorithms with their applications in bioinformatics. *Software Tools and Algorithms for Biological Systems*, 191–199.

Choat, B., Brodribb, T. J., Brodersen, C. R., Duursma, R. A., López, R., & Medlyn, B. E. (2018). Triggers of tree mortality under drought. *Nature, 558*, 531–539. https://doi.org/10.1038/s41586-018-0240-x

Christian, J. I., Hobbins, M., Hoell, A., Otkin, J. A., Ford, T. W., Cravens, A. E., ... & Mishra, V. (2024). Flash drought: A state of the science review. *Wiley Interdisciplinary Reviews: Water*, *11*, e1714.

Emaminejad, S. A., Sparks, J., & Cusick, R. D. (2023). Integrating bio-electrochemical sensors and machine learning to predict the efficacy of biological nutrient removal processes at water resource recovery facilities. *Environmental Science & Technology, 57*, 18372–18381.

EPA (n.d.). Coastal integrated forestry operations approvals, accessed 5 June 2025, < https://www.epa.nsw.gov.au/Your-environment/Native-forestry/Public-native-forestry/Integrated-Forestry-Operations-Approvals/Coastal-IFOA>

Gibson, R., Danaher, T., Hehir, W., & Collins, L. (2020). A remote sensing approach to mapping fire severity in south-eastern Australia using Sentinel-2 and random forest. *Remote Sensing of Environment*, *240*, 111702.

Gorelick, N., Hancher, M., Dixon, M., Ilyushchenko, S., Thau, D., & Moore, R. (2017). Google Earth Engine: Planetary-scale geospatial analysis for everyone. *Remote Sensing of Environment*, *202*, 18–27.

Hislop, S., Stone, C., Gibson, R. K., Roff, A., Choat, B., Nolan, R. H., ... & Carnegie, A. J. (2023). Using dense Sentinel-2 time series to explore combined fire and drought impacts in eucalypt forests. *Frontiers in Forests and Global Change*, *6*, 1018936.

Inbar, A., Nyman, P., Rengers, F. K., Lane, P. N., & Sheridan, G. J. (2018). Climate dictates magnitude of asymmetry in soil depth and hillslope gradient. *Geophysical Research Letters*, *45*(13), 6514–6522.

Ke, G., Meng, Q., Finley, T., Wang, T., Chen, W., Ma, W., Ye, Q., & Liu, T.-Y. (2017). LightGBM: A highly efficient gradient boosting decision tree. *Advances in Neural Information Processing Systems*, *30*.

Landsberg, J., & Waring, R. (2017). Water relations in tree physiology: Where to from here? *Tree Physiology, 37*(1), 18–32. https://doi.org/10.1093/treephys/tpw108

Landsberg, J., & Wylie, F. R. (1983). Water stress, leaf nutrients and defoliation: A model of dieback of rural eucalypts. *Australian Journal of Ecology*, *8*(1), 27–41. https://doi.org/10.1111/j.1442-9993.1983.tb01584.x

Leigh, A., Sevanto, S., Close, J. D., & Nicotra, A. B. (2017). The influence of leaf size and shape on leaf thermal dynamics: Does theory hold up under natural conditions? *Plant, Cell & Environment*, *40*(2), 237–248. https://doi.org/10.1111/pce.12857

Losso, A., Challis, A., Gauthey, A., Nolan, R. H., Hislop, S., Roff, A., ... & Choat, B. (2022). Canopy dieback and recovery in Australian native forests following extreme drought. *Scientific Reports*, *12*(1), 21608.

Lundberg, S. (2017). A unified approach to interpreting model predictions. *arXiv preprint*, arXiv:1705.07874.

McDougall, K. L., & Summerell, B. A. (2003). The impact of *Phytophthora cinnamomi* on the flora and vegetation of New South Wales—a reappraisal. In J. A. McComb, G. E. Hardy, & I. C. Tommerup (Eds.), *Phytophthora in forests and natural ecosystems: Proceedings of the 2nd International IUFRO Working Party* (pp. 49–56). Murdoch University Print.

McDowell, N. G., Sapes, G., Pivovaroff, A., Adams, H. D., Allen, C. D., Anderegg, W. R., ... & Cochard, H. (2022). Mechanisms of woody-plant mortality under rising drought, CO_2, and vapor pressure deficit. *Nature Reviews Earth & Environment*, *3*, 294–308.

Metzen, D., Sheridan, G. J., Benyon, R. G., Bolstad, P. V., Griebel, A., & Lane, P. N. (2019). Spatio-temporal transpiration patterns reflect vegetation structure in complex upland terrain. *Science of the Total Environment, 694*, 133551.

Nichols, E.R., Bendall, E.R., Peters J.M.R., Tissue D.T., Medlyn B.E., Choat, B (in prep) Extent of recovery from severe drought is dictated by post drought rainfall, long-term aridity and tree size.

Nicholls, N. (1991). The El Niño/Southern Oscillation and Australian vegetation. *Vegetatio, 91*, 23–36.

Nolan, R. H., Collins, L., Gibson, R. K., Samson, S. A., Rolls, K. T., Milner, K., ... & Boer, M. M. (2022). The carbon cost of the 2019–20 Australian fires varies with fire severity and forest type. *Global Ecology and Biogeography*, 31(10), 2131-2146.

Nolan, R. H., Lane, P. N., Benyon, R. G., Bradstock, R. A., & Mitchell, P. J. (2014). Changes in evapotranspiration following wildfire in resprouting eucalypt forests. *Ecohydrology, 7*(5), 1363–1377.

Nolan R.H., Gauthey A., Losso A., Medlyn B.E., Smith R., Chhajed, S.S., Fuller K., Song M., Li X., Beaumont L.J., Boer M.M., Wright I.J., Choat B. (2021). Hydraulic failure and tree size linked with canopy die-back in eucalypt forest during extreme drought. *New Phytologist* 230, 1354-1365

NSW DCCEEW. (2020). Fire Extent and Severity Mapping (FESM), accessed from The Sharing and Enabling Environmental Data Portal [https://datasets.seed.nsw.gov.au/dataset/33c2ee86-d2f7-4aaf-8c40-76b6d393a35c], date accessed 2025-03-25.

Qin, Y., Xiao, X., Wigneron, J. P., Ciais, P., Canadell, J. G., Brandt, M., ... & Moore, B. III. (2022). Large loss and rapid recovery of vegetation cover and aboveground biomass over forest areas in Australia during 2019–2020. *Remote Sensing of Environment, 278*, 113087.

Quan, X., Chen, R., Yebra, M., Riaño, D., Resco de Dios, V., Li, X., He, B., Nolan, R.H., Griebel, A., Boer, M.M., & Sun, Y. (2024). Sub-daily live fuel moisture content estimation from Himawari-8 data. *Remote Sensing of Environment, 308*.

Quan, X., Wang, W., Xie, Q., He, B., Resco de Dios, V., Yebra, M., Jiao, M., & Chen, R. (2023). Improving wildfire occurrence modelling by integrating time-series features of weather and fuel moisture content. *Environmental Modelling & Software, 170*.

Rhee, J., & Im, J. (2017). Meteorological drought forecasting for ungauged areas based on machine learning: Using long-range climate forecast and remote sensing data. *Agricultural and Forest Meteorology, 237*, 105-122.

Silver, M. J., & Carnegie, A. J. (2017). An independent review of bell miner associated dieback.
Trenberth, K. E., Dai, A., Van Der Schrier, G., Jones, P. D., Barichivich, J., Briffa, K. R., & Sheffield, J. (2014). Global warming and changes in drought. *Nature Climate Change*, *4*(1), 17–22.

Smith, M .G., Arndt, S. K., Miller, R. E., Kasel, S., & Bennett, L. T. (2018). Trees use more non-structural carbohydrate reserves during epicormic than basal resprouting. *Tree Physiology*, *38*(12), 1779-1791.

Vicente-Serrano, S. M., Beguería, S., & López-Moreno, J. I. (2010). A multiscalar drought index sensitive to global warming: the standardized precipitation evapotranspiration index. *Journal of climate*, *23*, 1696-1718.

Yebra, M., Quan, X., Riaño, D., Rozas Larraondo, P., van Dijk, A. I. J. M., & Cary, G. J. (2018). A fuel moisture content and flammability monitoring methodology for continental Australia based on optical remote sensing. *Remote Sensing of Environment, 212*, 260–272.

Yebra, M., Scortechini, G., Adeline, K., Aktepe, N., Almoustafa, T., et al. (2024). Globe-LFMC 2.0, an enhanced and updated dataset for live fuel moisture content research. *Scientific Data, 11*, 332.

6. Appendix 1. Additional Figures and Tables

Figures and tables referred to in the main body of the report.

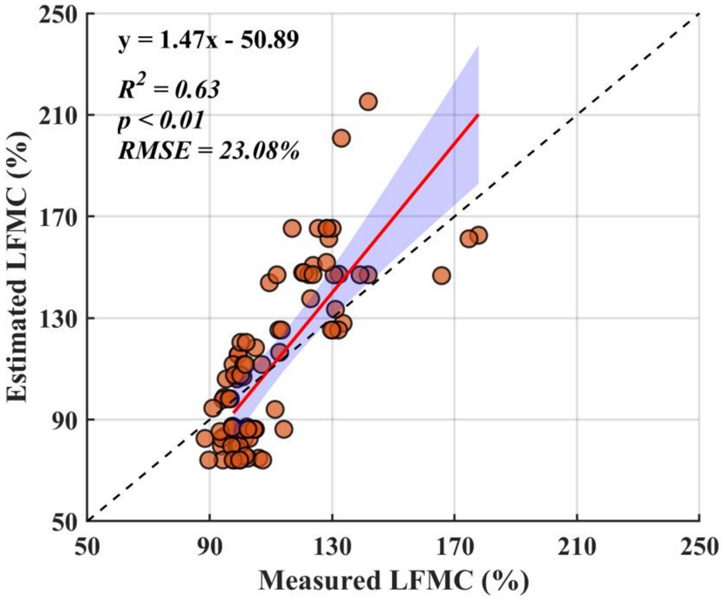

Figure A1. Live Fuel Moisture Content (LFMC) estimation based on remotely sensed data vs. measurements. Live Fuel Moisture Content measurements were taken from Globe-LFMC 2.0 (Yebra et al. 2024).

Yebra, M., Scortechini, G., Adeline, K., Aktepe, N., Almoustafa, T., et al. (2024). Globe-LFMC 2.0, an enhanced and updated dataset for live fuel moisture content research. *Scientific Data*, 11, 332.

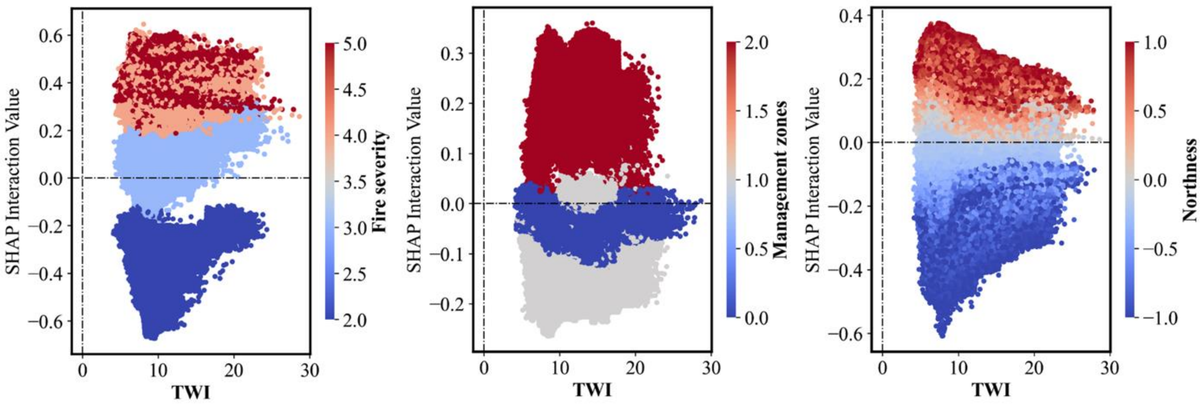

Figure A2. The interaction between TWI and Fire severity, Management zones, and Northness for the partial dead canopy case. Fire severity from 2 to 5 indicates the low, moderate, high, and extreme. Management from 0 to 2 indicated the conserved area, conserved forest, and harvested forest. Northness = 1 indicates north faced aspect and =0 indicates south faced aspect.

Table A1. Spatial Variable Dataset Sources and URLs

Factor	**Dataset**	**URL**
Conservation Areas	Collaborative Australian Protected Areas Database	https://fed.dcceew.gov.au/datasets/ec356a872d8048459fe78fc80213dc70_0/explore
State Forests	NSW Dedicated State Forests	https://data-fcnsw.opendata.arcgis.com/search
Hardwood Plantations	FCNSW Hardwood Plantation	https://data-fcnsw.opendata.arcgis.com/search
Vegetation Groups	Major Vegetation Groups and Subgroups - NVIS	https://www.dcceew.gov.au/environment/land/native-vegetation/national-vegetation-information-system
Fire Severity	Fire Extent and Severity Mapping (FESM)	https://datasets.seed.nsw.gov.au/dataset/fire-extent-and-severity-mapping-fesm
Terrain	Elevation (DEM)	https://portal.spatial.nsw.gov.au
Pest Risk	Bell Miner Associated Dieback	Dataset obtained from NSW DPI

7. Appendix 2. Canopy Health Score Protocol

Crown attributes and scoring system for canopy health scores for unburnt trees. Each crown attribute is summed, to produce a final canopy health score ranging from 0, for a dead tree with no leaves remaining, to 25 for a healthy tree. Scoring system modified from Stone et al. (2008).

Score	Brief description	Expanded description
Crown size		
5	Large, vigorous	Well-balanced, fully-extended crown, shaped by large branches containing a healthy 'hierarchy' of smaller branches supporting foliage
3	Moderate	Moderately-contracted crown, non-uniform in shape with foliage unevenly distributed. Approximately half of the outer, smaller branches dead or missing
1	Contracted	Crown contracted, all outer branches dead or missing, foliage on only major branches or stem arising from epicormic growth
0	Dead tree	No canopy
Crown density		
5	Very dense	Very dense leaf clumps with even distribution of clumps over the crown. Very little light penetrating the leaf clumps
4	Dense	Dense leaf clumps distributed unevenly over the crown
3	Moderate	Clumps of average density with reasonable distribution or dense clumps very unevenly spread
2	Sparse	Clumps are sparse and poorly spread
1	Very sparse	Very few leaves anywhere in crown
0	Dead tree	No canopy
Dead branches		
5	None	No visible dead branches or branchlets/shoots in the crown
4	Dead terminal shoots	On close inspection some dead terminal branches are evident but not over all the crown
3	Dead small branches	Some small branches are dead but not over all the crown. These are easily observed but do not give the impression of seriously affecting the crown
2	Dead main branches	Some large and or small branches dead over part of the crown with the obvious impression of serious branch death
1	Dead main branches	Large and small branches dead over most of the crown which is obviously dying
0	Dead tree	No canopy
Crown epicormic growth (indicates plant stress, with eucalypts frequently resprouting following disturbance)		
5	None	0 – 20% of canopy is epicormic in origin
4	Minor	20 – 40% of canopy is epicormic in origin
3	Moderate	40 – 60% of canopy is epicormic in origin
2	Extensive	60 – 80% of canopy is epicormic in origin
1	Severe	80 – 100% of canopy is epicormic in origin
0	Dead tree	No canopy
Leaf discolouration / browning (discoloured leaves were light grey-green in colour and were distinct from healthy foliage)		
5	None	No visible discolouration or browning
4	Minor	0 – 10% of canopy exhibits leaf browning and/or discolouration
3	Moderate	10 – 50% of canopy exhibits leaf browning and/or discolouration
2	Extensive	50 – 100% of canopy is discoloured, +/- leaf browning
1	Severe	All of canopy is brown
0	Dead tree	No canopy

References

Stone, C., Kathuria, A., Carney, C. and Hunter, J., 2008. Forest canopy health and stand structure associated with bell miners (*Manorina melanophrys*) on the central coast of New South Wales. *Austral. For.*, 71(4): 294-302, 10.1080/00049158.2008.106750

8. Appendix 3. Canopy Dieback Area Statistics

Table A2. Area (ha) classified for each canopy dieback class within spatial variables BMAD, Fire Severity, and Management Zone. Fire severity classes were derived from Fire Extent and Severity Mapping (FESM) (NSW DCCEEW, 2020). Management zones are defined as Conserved area (protected areas including National Parks and Reserves) Conserved forest (State Forest areas managed for conservation including Forest Management Zones 1-3B) and Harvest forest (State Forest areas managed for harvest, Forest Management Zone 4).

Variable	Category	Canopy Dieback Class Area 2023-10 (ha)		
		Dead canopy	**Partial dead canopy**	**Live canopy**
BMAD Value	**No BMAD**	14160	148407	245347
	BMAD	299	1772	1890

Variable	Category	Canopy Dieback Class Area 2023-10 (ha)		
		Dead canopy	**Partial dead canopy**	**Live canopy**
Fire Severity	**Low**	1512	13506	43689
	Moderate	2056	27844	53226
	High	1937	18553	17964
	Extreme	2464	12934	9085
	NoData	6491	77342	123272

Variable	Category	Canopy Dieback Class Area 2023-10 (ha)		
		Dead canopy	**Partial dead canopy**	**Live canopy**
Management zones	**Conserved area**	8711	83102	146302
	Conserved forest	1728	15668	37563
	Harvest forest	4021	51408	63372

Table A3. Area (ha) classified for each canopy dieback class within spatial variables BMAD and Fire Severity for Conserved area (protected areas including National Parks and Reserves) Management Category.

Conserved area		Canopy Dieback Class Area 2023-10 (ha)		
Variable	Category	**Dead canopy**	**Partial dead canopy**	**Live canopy**
BMAD Value	**No BMAD**	7245	69481	122720
	BMAD	110	687	863

Conserved area		Canopy Dieback Class Area 2023-10 (ha)		
Variable	Category	**Dead canopy**	**Partial dead canopy**	**Live canopy**
Fire Severity	**Low**	1047	8362	27218
	Moderate	1241	16462	30099
	High	995	9656	8534
	Extreme	1355	6098	3697
	NoData			

Table A4. Area (ha) classified for each canopy dieback class within spatial variables BMAD and Fire Severity for Conserved Forest (State Forest areas managed for conservation including Forest Management Zones 1-3B) Management Category.

Conserved forest		Canopy Dieback Class Area 2023-10 (ha)		
Variable	Category	**Dead canopy**	**Partial dead canopy**	**Live canopy**
BMAD Value	**No BMAD**	1415	12992	31380
	BMAD	47	250	349

Conserved forest		Canopy Dieback Class Area 2023-10 (ha)		
Variable	Category	**Dead canopy**	**Partial dead canopy**	**Live canopy**
Fire Severity	**Low**	88	1403	5171
	Moderate	203	2917	7597
	High	272	1984	2694
	Extreme	353	1594	1380
	NoData			

Table A5. Area (ha) classified for each canopy dieback class within spatial variables BMAD and Fire Severity for Harvest Forest (State Forest areas managed for harvest, Forest Management Zone 4) Management Category.

Harvest forest		Canopy Dieback Class Area 2023-10 (ha)		
Variable	Category	**Dead canopy**	**Partial dead canopy**	**Live canopy**
BMAD Value	**No BMAD**	3303	42866	53161
	BMAD	96	560	385

Harvest forest		Canopy Dieback Class Area 2023-10 (ha)		
Variable	Category	**Dead canopy**	**Partial dead canopy**	**Live canopy**
Fire Severity	**Low**	141	1643	4510
	Moderate	294	4137	7264
	High	371	4023	3957
	Extreme	371	3227	2611
	NoData			

Table A6. Proportion (%) of total area classified for each canopy dieback class and proportion within spatial variables BMAD, Fire Severity, and Management Zone categories. Fire severity classes were derived from Fire Extent and Severity Mapping (FESM) (NSW DCCEEW, 2020). Management zones are defined as Conserved area (protected areas including National Parks and Reserves) Conserved forest (State Forest areas managed for conservation including Forest Management Zones 1-3B) and Harvest forest (State Forest areas managed for harvest, Forest Management Zone 4).

		Proportion of Total			**Proportion Within Category**		
Variable	Category	**Dead canopy**	**Partial dead canopy**	**Live canopy**	**Dead canopy**	**Partial dead canopy**	**Live canopy**
BMAD Value	**No BMAD**	3.44%	36.03%	59.57%	3.47%	36.38%	60.15%
	BMAD	0.07%	0.43%	0.46%	7.56%	44.73%	47.71%

		Proportion of Total			**Proportion Within Category**		
Variable	Category	**Dead canopy**	**Partial dead canopy**	**Live canopy**	**Dead canopy**	**Partial dead canopy**	**Live canopy**
Fire Severity	**Low**	0.37%	3.28%	10.61%	2.58%	23.01%	74.42%
	Moderate	0.50%	6.76%	12.92%	2.47%	33.50%	64.03%
	High	0.47%	4.50%	4.36%	5.04%	48.25%	46.72%
	Extreme	0.60%	3.14%	2.21%	10.06%	52.83%	37.11%
	NoData	1.58%	18.78%	29.93%	3.13%	37.34%	59.52%

		Proportion of Total			**Proportion Within Category**		
Variable	Category	**Dead canopy**	**Partial dead canopy**	**Live canopy**	**Dead canopy**	**Partial dead canopy**	**Live canopy**
Management zones	**Conserved area**	2.11%	20.18%	35.52%	3.66%	34.90%	61.44%
	Conserved forest	0.42%	3.80%	9.12%	3.14%	28.51%	68.35%
	Harvest forest	0.98%	12.48%	15.39%	3.38%	43.27%	53.34%

Table A7. Proportion (%) of total area classified for each canopy dieback class and proportion of area for spatial variables BMAD, Fire Severity with Conserved area (protected areas including National Parks and Reserves) Management Category.

Conserved area		**Proportion of Total**			**Proportion Within Category**		
Variable	Category	**Dead canopy**	**Partial dead canopy**	**Live canopy**	**Dead canopy**	**Partial dead canopy**	**Live canopy**
BMAD Value	**No BMAD**	3.60%	34.55%	61.02%	3.63%	34.84%	61.53%
	BMAD	0.05%	0.34%	0.43%	6.62%	41.38%	52.00%

Conserved area		**Proportion of Total**			**Proportion Within Category**		
Variable	Category	**Dead canopy**	**Partial dead canopy**	**Live canopy**	**Dead canopy**	**Partial dead canopy**	**Live canopy**
Fire Severity	**Low**	0.91%	7.29%	23.72%	2.86%	22.83%	74.31%
	Moderate	1.08%	14.34%	26.23%	2.60%	34.44%	62.97%
	High	0.87%	8.41%	7.44%	5.19%	50.33%	44.48%
	Extreme	1.18%	5.31%	3.22%	12.16%	54.69%	33.15%

Table A8. Proportion (%) of total area classified for each canopy dieback class and proportion of area for spatial variables BMAD, Fire Severity with Conserved forest (State Forest areas managed for conservation including Forest Management Zones 1-3B) Management Category.

Conserved forest		**Proportion of Total**			**Proportion Within Category**		
Variable	Category	**Dead canopy**	**Partial dead canopy**	**Live canopy**	**Dead canopy**	**Partial dead canopy**	**Live canopy**
BMAD Value	**No BMAD**	3.05%	27.98%	67.58%	3.09%	28.37%	68.54%
	BMAD	0.10%	0.54%	0.75%	7.21%	38.75%	54.04%

Conserved forest		**Proportion of Total**			**Proportion Within Category**		
Variable	Category	**Dead canopy**	**Partial dead canopy**	**Live canopy**	**Dead canopy**	**Partial dead canopy**	**Live canopy**
Fire Severity	**Low**	0.34%	5.47%	20.16%	1.32%	21.06%	77.62%
	Moderate	0.79%	11.37%	29.61%	1.90%	27.22%	70.89%
	High	1.06%	7.73%	10.50%	5.49%	40.08%	54.42%
	Extreme	1.37%	6.21%	5.38%	10.60%	47.92%	41.48%

Table A9. Proportion (%) of total area classified for each canopy dieback class and proportion of area for spatial variables BMAD, Fire Severity with Harvest forest (State Forest areas managed for harvest, Forest Management Zone 4) Management Category.

Harvest forest		**Proportion of Total**			**Proportion Within Category**		
Variable	Category	**Dead canopy**	**Partial dead canopy**	**Live canopy**	**Dead canopy**	**Partial dead canopy**	**Live canopy**
BMAD Value	**No BMAD**	3.29%	42.71%	52.96%	3.33%	43.16%	53.52%
	BMAD	0.10%	0.56%	0.38%	9.22%	53.81%	36.97%

Harvest forest		**Proportion of Total**			**Proportion Within Category**		
Variable	Category	**Dead canopy**	**Partial dead canopy**	**Live canopy**	**Dead canopy**	**Partial dead canopy**	**Live canopy**
Fire Severity	**Low**	0.43%	5.05%	13.86%	2.24%	26.10%	71.66%
	Moderate	0.90%	12.71%	22.32%	2.51%	35.38%	62.11%
	High	1.14%	12.36%	12.16%	4.44%	48.18%	47.38%
	Extreme	1.14%	9.91%	8.02%	5.98%	51.97%	42.05%